Estimation of Car-following Safety: Application to the Design of Intelligent Cruise Control

by

SHIH-KEN CHEN

B.S. in Agricultural Machinery Engineering
National Taiwan University
(1985)

M.S. in Mechanical Engineering
University of Wisconsin-Madison
(1990)

Submitted to the Department of Mechanical Engineering

in partial fulfillment of the requirements for the degree of

DOCTOR OF PHILOSOPHY IN MECHANICAL ENGINEERING

at the

MASSACHUSETTS INSTITUTE OF TECHNOLOGY

February 1996

Author .....
Department of Mechanical Engineering
November 30, 1996

Certified by .....
Thomas B. Sheridan
Thesis Supervisor

Accepted by .....
Ain A. Sonin
Chairman, Departmental Committee

Estimation of Car-following Safety:

Application to the Design of Intelligent Cruise Control

by

SHIH-KEN CHEN

Submitted to the Department of Mechanical Engineering

on November 30, 1996, in partial fulfillment of the
requirements for the degree of
DOCTOR OF PHILOSOPHY IN MECHANICAL ENGINEERING

Abstract

In designing an intelligent cruise controller (ICC) for an automobile, one would like to know the risk of collision based on all the information provided by on-board sensors and computers as well as vehicle, highway and driver conditions. Based on this information, the ICC can determine whether to take actions and what kind of actions. Most current ICC's use radar to detect speed and distance of the two vehicles and determine the control action based on a theoretical safe-following model without taking into account other factors such as the individual driver's driving behavior. As a result, these ICC's, when they are put in the market, may not be acceptable for all drivers.

The purpose of this thesis was to investigate differences in car-following behavior under different conditions, to develop a framework for modelling car-following safety based on these real data, and finally to demonstrate the usefulness of this model in the design of intelligent cruise control.

Two approaches were used to measure car-following behavior: field measurements and simulator experiments. The field measurements provided realistic but uncontrolled data for a large and varied population under different environmental conditions. The simulator experiments, on the other hand, provided data among different groups of drivers in a planned, controlled environment. The results show that environmental effects on car-following were mostly minimum, while driver characteristics have a great influence on car-following behavior.

A preliminary analysis of the kinematics of car-following safety was presented. The analysis showed that an analytical solution for this safety model might not be obtainable due to the fact that the empirical car-following data could not be expressed in a convenient analytical form. We proposed an alternative solution to this problem by using the Monte-Carlo simulation to determine the probabilities of a crash occuring given certain specified conditions. A fuzzy-logic intelligent cruise controller was then developed based on the crash analysis results from the model. Simulation results showed that such an ICC has potential of reflecting individual driver's driving habits and, at the same time, maintaining safety.

Thesis Committee: Professor Thomas B. Sheridan (Chairman)
Professor Moshe E. Ben-Akiva
Professor Louis L. Bucciarelli, Jr.

Acknowledgments

I would like to express my deepest gratitude to my thesis advisor, Professor Thomas B. Sheridan for his constant support and encouragement throughout my doctoral study at MIT. His patient guidance and inspiring advice help me through many difficult moments. I would also like to thank my thesis committee members, Professor Moshe E. Ben-Akiva and Professor Louis L. Bucciarelli, Jr., for their invaluable help and interest in my work.

The companionship and technical support I received while working in the Human-Machine Systems Laboratory are most enjoyable and precious experience. I am especially grateful to Dr. Jie Ren for sharing his experience and technical expertise when I needed them, to Nicholas Patrick for his help in statistical analysis, to Jienjuen Hu and Shiet Sheng Chen for their inputs to the building of HMSL driving simulator, to the three UROP students, Steven Ahn, Miltos Kambourides and Mithran Mathew, for their efforts in collecting highway data for the project, and to Jackie Anapole and Walter Milne for recruiting many subjects for the experiements. Many thanks to all the HMSL members for their lasting friendship and support: Dave Schloerb, Shumei Askey, Suyeong Kim, James Thomas, Mark Ottensmeyer, Mike Kilaras. Sincere thanks also extend to former members of the lab: Chi-Cheng Cheng, Kan-Ping Chin, Mike Massimino and Jong Park. I would also like to thank all the subjects for their participation in this research.

The financial support of the Toyota Motor Corporation is deeply appreciated. I would like to thank Mr. Norio Komoda and Hideki Kusunoki for the insight discussion about this sponsored project.

My parents, Shih-Man Chen and Jie-Jien Chen have given me endless love, support and confidence throughout the long doctoral work. I will always be grateful for their unequivocal love and for accepting the long separation.

Last but not least, I would like to express my heartfelt thanks to my wife, Yu-Mei Wang, for her continuous love and encouragement when I was down and for the sacrifice and understanding during very difficult times.

Contents

List of Figures

List of Tables

Chapter 1

INTRODUCTION

1.1 Problem Description

Rear-end collision is one of the most common types of crashes involving two or more vehicles. The National Safety Council (NSC) reported [1] that there were approximately 11.5 million automobile crashes in 1990, of which 2.2 million were front-to-rear-end, about 19.1% of the total. These crashes accounted for 24% of all collisions involving two or more vehicles. The NSC further reported, in the same year, on 1800 fatalities (in front-to-rear-end crashes) or 4.4% of the fatalities occurring in all motor vehicle crashes. Front-to-rear-end collisions accounted for 11.4% of all fatalities involving two or more vehicles in crashes [2].

There is plenty of evidence that these front-to-rear-end accidents result primarily from drivers keeping inadequate headway for the speed of travel and, therefore, not being able to stop or slow down sufficiently when the lead vehicle unexpectedly de-

celerates or stops rapidly due to the late timing of a maneuver, an obstacle, or some other emergency situation. The NSC [1] reported that 8.7% of all collisions or nearly one-half of front-to-rear-end crashes are due to drivers following too closely. Various warning systems and intelligent cruise controllers are being designed to help the inattentive, inexperienced or risk-prone driver keep an adequate following distance and react when unexpected situations occur. To be acceptable to the driver, those devices should be actuated by a "smart" algorithm which activates either or both warning and deceleration, depending on the circumstances. Unfortunately, what drivers believe to be an acceptable following distance is not easy to deal with for many reasons. The individual driver has his/her own intuitive and heuristic internal model of the car following situation. The driver may also decide to engage in active risk-taking behavior when planning and carrying out driving maneuvers. The driver's sensory and perceptual limits for detecting speed and distance may change according to age and gender. These and many other factors are not mutually exclusive, which makes the defining of a safe following distance very complex.

The current research on "car-following" focuses on fitting overall highway data to some theoretical model. This approach usually includes data for every car in a traffic stream, some of which are not really car-following. In order to realize a valid car-following model, an experimental data for steady car-following needs to be established, and for this a method to evaluate the car-following safety needs to be developed.

1.2 Car-following Research

Considerable research has been directed to drivers' car-following behavior or headway distribution. Tolle [3] compared different models of headway distribution using real highway data. He tested three different statistical distributions, composite exponential, Pearson Type III and log-normal , and concluded that log-normal was the best fit of the three. Koshi [4] suggested possible dual-mode car-following behavior. He analyzed highway data and found the possible discontinuity between low speed and high speed region. Chishaki [5] formulated a headway distribution model based on the distinction between leaders and followers. He developed a very complex mathematical model to describe an overall headway distribution as a function of traffic flow.

Several researchers also tried to define a so-called "safe" following distance (or headway). Dull [6] defined the safe distance as a function of vehicle braking capability and of driver reaction time. He employed this theoretical safe stopping distance as a safe following distance in his design of collision warning system. Colbourn [8] investigated the effects of traveling speed, driving experience and instructed probability of the leading vehicle's stopping on driver car-following behavior. He found that the effects were minimum, and that drivers adopt headways of approximately two seconds. Fenton [9] proposed a headway safety policy for automated highway operations by analyzing all the possible parameters that affect the theoretical stopping distance. Ioannou [7] et al. used the California rule for safe car-following distance, a vehicle length for every 10 m.p.h, for their intelligent cruise control design.

These mathematical models, though easy to implement in simulation, can hardly reflect the real driver judgments of the safe following distances, since they all try to define what is a safe following distance instead of what following distances drivers believe to be safe and/or actually employ.

1.3 Intelligent Cruise Control

An Intelligent Cruise Control (ICC) system is an assisting system that controls relative speed and distance between two vehicles in the same lane. The system has great potential for enhancing the safety, comfort and convenience of highway driving by sensing and appropriately responding to forward traffic scenarios. A schematic diagram for the ICC system is shown in figure 1-1.

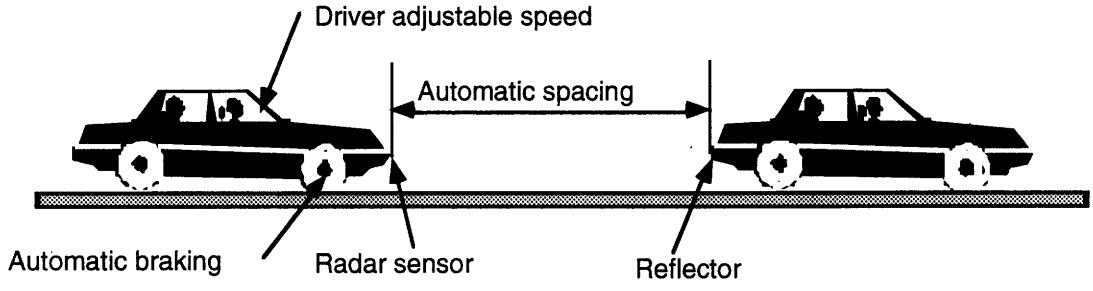

Figure 1-1: Intelligent Cruise Control Operating Concept

Highway driving safety is potentially improved by responding to slower leading vehicles with high closure rates and vehicles that cut into the lane of the intelligent cruise control vehicle. High closure rate traffic scenarios detected by the system alert the driver and automatically initiate braking. The degree of braking depends on the

relative distance, own vehicle speed, and the closing rate.

Many automobile companies and research institutes have undertaken research and development of intelligent cruise control for the last few decades. Early research used warning devices to passively warn drivers of potential danger, instead of the active braking device that will automatically slow the vehicle in the presence of danger [6] [10]. The application of advanced technology sensors, processors and software has pushed forward to include braking control as part of the intelligent cruise control [11] [12] [13] [14].

1.4 Summary of this Thesis

1.4.1 Objectives

The objectives of this research are to develop a measurement method and experimental data for car-following, to evaluate car-following safety with a proposed simulation model, and to use such model to help design intelligent cruise control. For this purpose, the following issues are investigated:

1. Car-following behavior of Boston drivers.

2. Braking reaction time measured in a laboratory setting.

3. Safety model of car-following based on car-following behavior and braking reaction time.

4. Possible application to the design of intelligent cruise control.

This research first investigated constant velocity car following behavior as a function of absolute speed, weather, illumination, traffic density, driver intention, experience and gender. Two approaches were used to measure the car-following behavior: field measurements and actual-driver-in-the-loop simulator tests. The field measurements provided realistic but uncontrolled data for a large and varied population under different environmental conditions. The simulator tests, on the other hand, provided data distinguishing among different groups of drivers in a planned, controlled environment. Those data were then used in combination to develop and validate an evaluation model of car-following safety. Finally, with this knowledge of car-following safety, an example of intelligent cruise control is demonstrated.

1.4.2 Thesis Contributions

This thesis makes the following major contribution:

1. **A data base for steady car-following was acquired.** This data base provides analyzed steady car-following data instead of commonly seen raw data that includes much non-following information.

2. **A driving simulator was developed for investigation of driver behavior.** The low-cost, fixed-base driving simulator developed for this research provides a useful tool for further driver related research.

3. **A dynamic braking reaction time distribution was obtained.** Using the driving simulator to test driver braking reaction time proved to be safe, efficient and, we believe, reasonably accurate. With the control environment, both surprise and alert reaction time was investigated.

4. **A model for estimating car-following safety was implemented.** This thesis proposes the implementation of a Monte-Carlo model for evaluating car-following safety. The simulation demonstration shows its effectiveness in investigating safety under different conditions.

5. **A fuzzy intelligent cruise controller was developed using the safety simulation results.** It is first such design to take into account real driver car-following behavior. It improves the acceptability of this type of driver aid device.

1.4.3 Thesis Overview

This thesis is arranged as follows:

Chapter 2 presents the method used to collect and analyze highway data. The implication of environmental effects on car-following behavior are also discussed. In chapter 3, design of the Human-Machine Systems Laboratory (HMSL) Driving Simulator is first discussed. Experimental tasks for car-following and braking reaction measurement are then described. Chapter 4 discusses the model for evaluating car-following safety with some examples. Chapter 5 demonstrates the use of safety results in the development of a fuzzy intelligent cruise controller. Chapter 6 states the con-

clusions and suggests some directions for future research.

Chapter 2

Field Measurements on Car Following

Real highway data are important for evaluating the safety of driver car-following behavior and the effectiveness of intelligent cruise control. This chapter summarizes the locations chosen for highway measurements, describes the method used to obtain data from the measurements, and finally discusses the measurement results which imply environmental effects on car-following behavior, including effects of weather, illumination, traffic density and locations.

2.1 Location

The considerations for choosing the locations includes: being within convenient distance from MIT, high traffic density to measure steady car-following behavior, and availability of a high-rise building nearby for videotaping the traffic.

Most measurements were carried out on Interstate I-93 near Boston area. This section of I-93 is a dual three-lane freeway going north and south. The location has the merit of having steady traffic flow during the rush hour and even during the non-rush hour. Only data from the inner two lanes were taken. A high elevated parking lot along the highway was chosen to place a video camera so that we could have a clear view of the whole highway and thus were able to distinguish between vehicles on adjacent lanes. Figure 2-1 shows a typical view of the traffic on this section of highway.

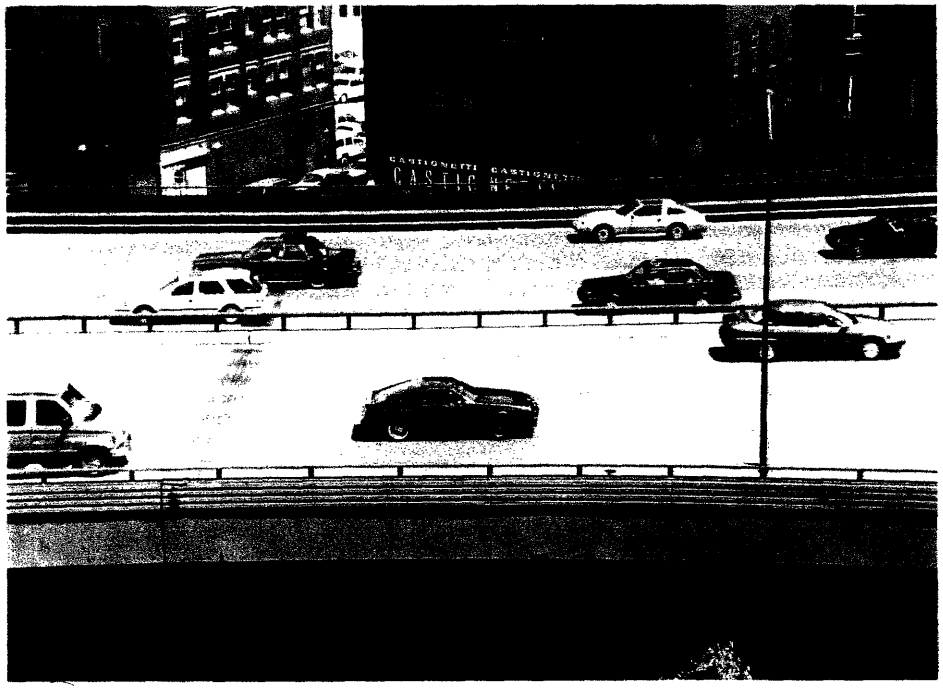

Figure 2-1: Typical View of the Traffic on I-93

Another location, the Massachusetts Turnpike (I-90), was mainly used to collect additional high speed data and to show the effect of a different location. This section of I-90 is a dual four-lane toll highway going east and west. Again, only the inner

two lanes were considered.

Both highways are well maintained and have good surface quality. The average throughput ranges from 1500 to 2000 vehicles per hour per lane during rush hour and approximately 1000 to 1600 vehicles per hour per lane during non-rush hour.

2.2 Variables

Clearly car-following spacing is a function of driver, environment and vehicle. In this thesis, however, only environmental conditions were considered for the field measurements since the other two variables are not readily measured from the method used to collect the traffic data. Instead, they will be considered in the simulator tests and safety evaluation sections. The environmental variables of interest for this thesis include:

1. Surface conditions - dry or wet,
2. Lighting conditions - daylight or night,
3. Traffic density - rush hour or non-rush hour, and
4. Location - near downtown area (I-93) or away from downtown (I-90).

Surface condition coincides with weather in that wet surface was considered only when there was light rain, the road surface was wet and the visibility was not much worst than that under dry surface. Daylight was considered to be normal light, with

no cars having their headlights on. Night was when all cars had their headlights on, and the sun had completely set. We defined the rush hour as 5 to 7 in the evening. The two locations were used to show whether drivers followed cars differently near downtown areas. These variables were chosen because they were easily observed and distinguished.

2.3 Data Collection and Analysis

A Sony Hi-8 Handycam video camcorder was used for measurement. It had a 10:1 zoom lens with 1 lux light sensitivity. The camera was adjusted so that about three cars following one another could be seen in one video frame. This ensured proper car-following action but did not sacrifice accuracy. The traffic data collected from the highways were analyzed using the stop-frame method on a VCR (distance measured by a scale on the screen). The VCR had a slow-frame speed of 1/60 second per frame, and this was used to calculate a velocity for the vehicles.

Since this study only considered car-following under a steady traffic stream, cars with observable acceleration/deceleration were discarded. To achieve this goal without measuring the acceleration rate, we employed the data only when there were at least three cars following each other at approximately the same speed. Two stationary marks, 55 feet apart on the highway, were used to calibrate between the distance that appears on the TV display (TV-screen-inches) and the distance on location (real distance). In order to avoid errors caused by image distortion from the camera, we measured the distance from the center of the screen where the markers were observed.

Each cited instance of car-following was classified by the speed at which both cars were traveling and the distance the cars were measured to be apart from one another. It was assumed and afterward checked that both cars were traveling at the same speed. It was also assumed that the velocity was constant for the specified distance between the two marks. A collection of about 50-100 of these data points constituted one data set for each video session. There were 60 video sessions from I-93 and 15 sessions from I-90, or roughly 5600 data points in all.

2.4 Results

The results of the field measurements are discussed in this section. Analysis of variance was used to evaluate the difference in car-following distances under different environmental conditions and so-called box plots provided graphical presentation of the comparisons and showed the general distributions. Figure 2-2 shows a typical example of a box plot. A box plot has several graphic elements. The lower and upper lines of each "box" are the 25th and 75th percentiles of the distribution. The line in the middle of the box is the median value of the sample. The lines extending above and below the box show the total range of data in the sample, except that any sample value that is more than 1.5 times the box range is shown as individual point above or below the box.

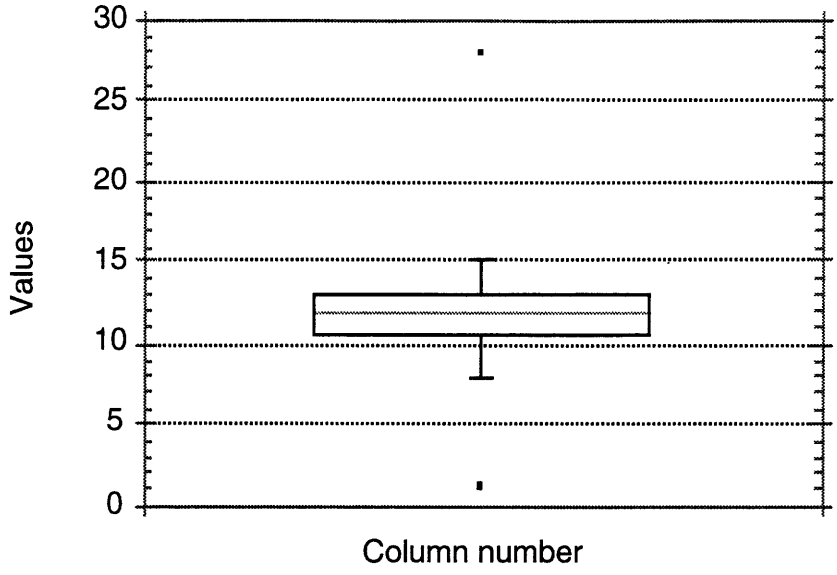

Figure 2-2: Typical Example of Box Plot

2.4.1 Baseline Results

Figure 2-3 shows the raw data under seven different conditions. Note that figure 2-3(a) to (e) are the raw data taken from I-93 while figure 2-3(f) and (g) are from I-90. Also note that only one non-rush hour data set, figure 2-3(b), is presented for comparison.

By observation, all the data sets seem to indicate that there is poor correlation between following distance and speed. A two-variable regression analysis was used to test this observation. The equation to be estimated under the analysis is

$$(following\ distance) = A + B * (speed) \tag{2.1}$$

where A and B are two coefficients to be estimated.

The results of the regression analysis are shown in Table 2.1. Since the sample

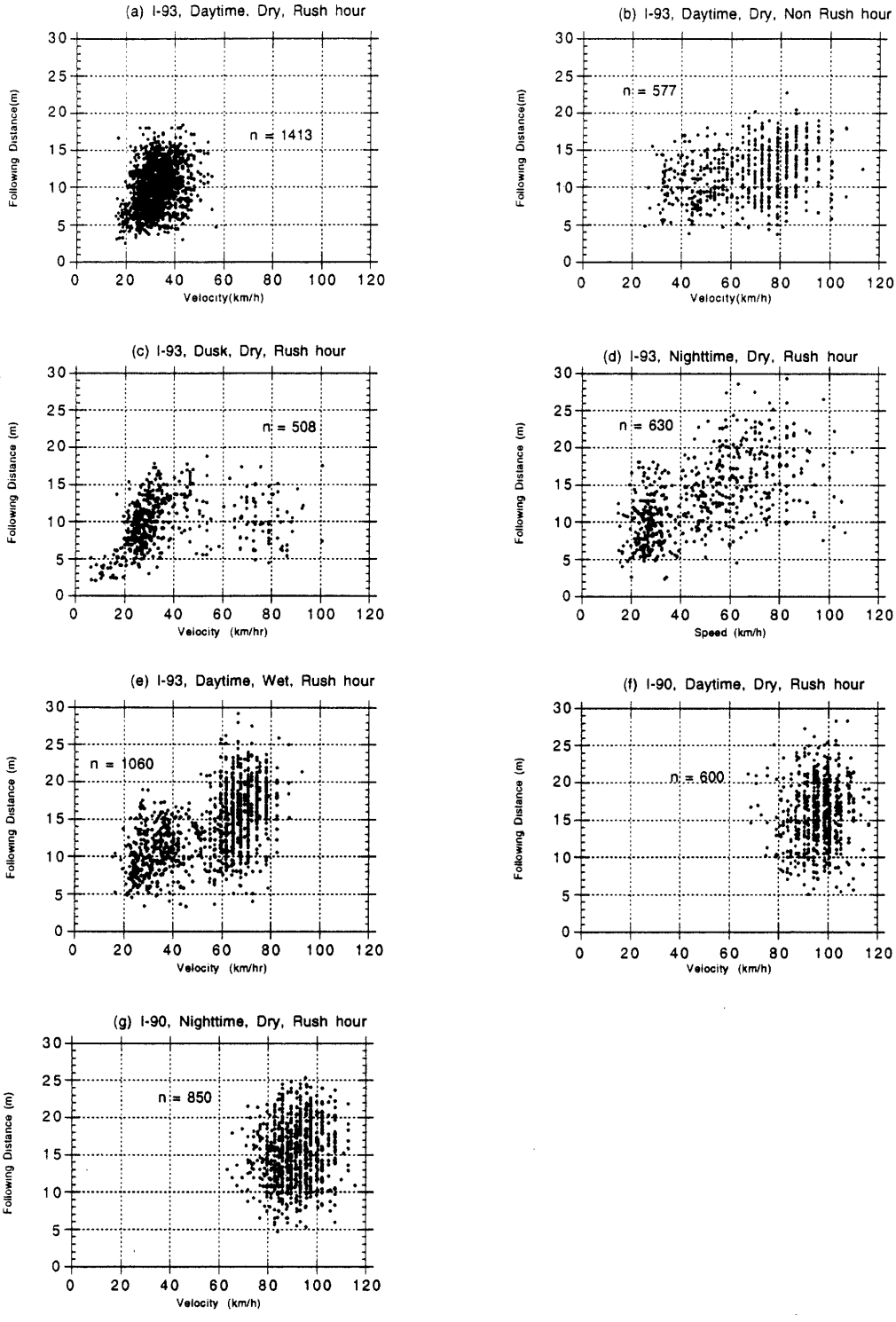

Figure 2-3: Raw Data

size is large enough, the Student's t test was used to determine whether A or B were significantly different from zero. This hypothesis could be rejected in both cases at the 95 percentile. The small R^2 values (< 0.4) show that there is little correlation within each data set.

	Coefficients			
Conditions	*Intercept, A*	*Slope, B*	R^2	*Number of Points*
I93, daytime, dry, rushhour	5.18	0.15	0.11	1413
I93, daytime, dry, nonrushhour	8.01	0.06	0.11	577
I93, dusk, dry, rushhour	8.28	0.046	0.069	508
I93, nighttime, dry, rushhour	6.28	0.14	0.35	610
I93, daytime, wet, rushhour	5.77	0.15	0.31	1060
I90, daytime, dry, rushhour	11.95	0.04	0.006	1600
I90, nighttime, dry, rushhour	10.19	0.06	0.015	850

Table 2.1: Regression Analysis for Following Distance vs. Speed

A "dual-mode" assumption is widely used in the analysis of traffic flow. It seemed to the author that car-following behavior might show a similar characteristic. A dual model is clearly evident in figure 2-3(c) and (e). The high speed region (or free-flow region) has a steeper slope than the low speed region (or congested region). The critical speed is at around 50 km/hr for both cases. Our interpretation of this phenomenon is that in the congested condition drivers do not really follow the cars ahead as closely as they would in a free-flow condition, because they know that they are not really in a steady flow and they will be forced to brake sooner or later. The non-rush hour data, on the other hand, do not show the "dual mode" characteristic and reveal only very slight variation within the whole speed range. The data also show a great variation among drivers in keeping a steady car-following distance. For

example, the following distance for the speeds of 40-50 km/hr ranges from 5 to 20 meters during daytime and from 5 to 25 meters during nighttime.

Figure 2-4 presents the raw data from Figure 1 in cumulative probability functions. From these graphs it is easy to see that people are more sensitive to speed during rush hour than during non rush hour. For example, under daylight and during rush hour, the average increase of following distance per speed increase of 10 km/hr was about one meter, while during non rush hour the average increase was only 0.6 meter. Notice the extremely narrow range for the non-rush hour data. This shows that drivers paid little attention to the their speeds when following the lead car under light traffic. It also appears that people were less sensitive to speed in car following when driving on I-90 than on I-93.

Another common way of dealing with car-following behavior is to look at the time headway distribution. A time headway is time needed for the following car to reach the *current* position of the lead car. In another word, the time headway is product of *current* relative distance between two cars and the inverse of following car *current* speed. A common recommendation from the government regarding highway safety is to follow a car with two seconds time headway. Figure 2-5 shows the histogram of time headway distribution for the daytime data. It is evident that majority of people we observed followed cars at much smaller time headway. In fact, most people seemed to keep one second headway. The overall distribution fits to a general log-normal distribution as suggested by many researchers [3] [15].

Figure 2-4: Raw Data in Percentile

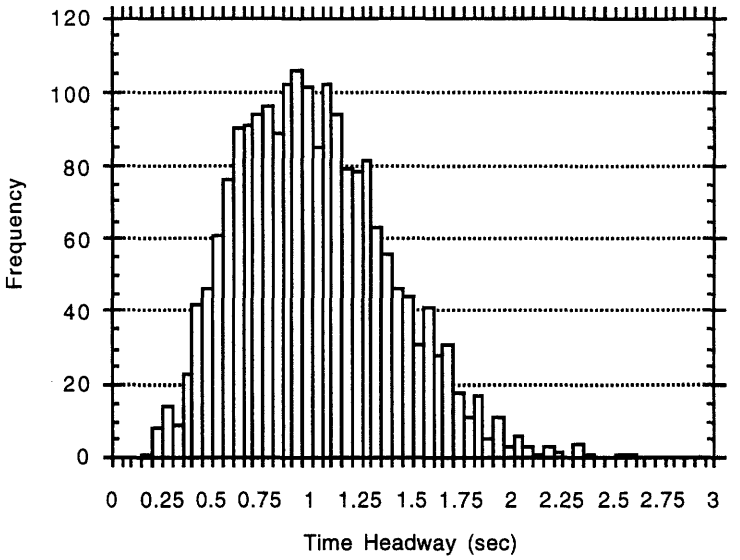

Figure 2-5: Histogram of Daytime Headway

2.4.2 Effect of Environmental Conditions

Based on the collected data, the car-following distance was found to vary greatly in each speed range.

Effect of Road Surface Conditions and Weather

Figure 2-6 compares driving on a dry surface in clear weather with driving on a wet surface in rainy weather. Generally speaking, people claim to take more caution while driving under adverse weather conditions than under normal conditions. (The effect of the road surface was considered to coincide with that of the weather since we did not collect other wet-pavement data such as icy road or snowy weather.) In our experiments, however, the average following distance was not significantly greater on rainy days than under clear weather for some of the speed ranges. An Analysis of Variance (ANOVA) showed that there were no statistically significant differences

between means for different conditions for the speed ranges from 40 to 60 km/hr, while the effect was significant for the ranges from 10 to 40 km/hr. Table 2.2 shows the detailed analysis. The results suggest that people may not be so sensitive to speed if the traffic flow is close to steady even though the pavement is wet. Note that also shown in figure 2-6 are the one-second and two-second headway lines. It is evident that most people keep well below the recommended two seconds headway, and many, especially at high speeds, are even below one second headway.

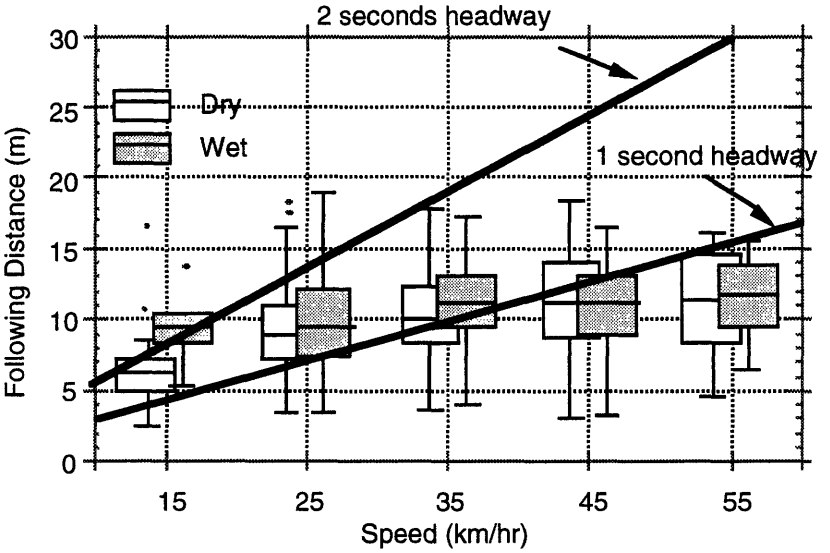

Figure 2-6: Comparison of Following Distance under Dry and Wet Road Surface

$SpeedRange(km/h)$	F	$d.f$	P
$10-20$	112.2	$1,40$	< 0.001
$20-30$	9.2	$1,681$	$= 0.0025$
$30-40$	9.1	$1,849$	$= 0.0026$
$40-50$	0.005	$1,275$	$= 0.94$
$50-60$	0.025	$1,105$	$= 0.874$

Table 2.2: ANOVA of Effect of Road Surface Conditions

Effect of Lighting Conditions

Figure 2-7 shows the effects of ambient lighting conditions on the car-following distance distribution. Due to the lack of high speed data for daytime on I-93, only those data under congested flow were compared. To examine the effect at higher speed, data from I-90 were used. This is justified since the effect of location is minimum as will be shown later. We would normally expect that low visibility will greatly increase the following distance. An ANOVA was again computed and the results are shown in Table 2.3. The car-following differences between daytime and nighttime were significant for the low speed region while there is no significant difference for the high speed region. Overall, the car-following distance during nighttime was approximately 14 percent greater than that during daytime.

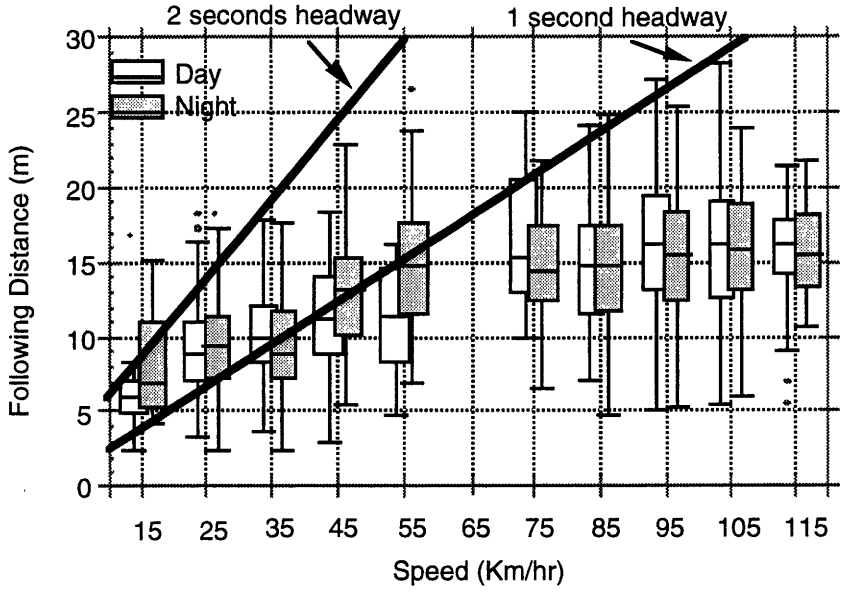

Figure 2-7: Comparison of Following Distance during Day and Night

$SpeedRange(km/h)$	F	$d.f$	P
$10-20$	4.98	$1,53$	$=0.03$
$20-30$	4.74	$1,736$	$=0.03$
$30-40$	3.32	$1,783$	$=0.07$
$40-50$	18.65	$1,290$	<0.001
$50-60$	36.86	$1,171$	<0.001
$70-80$	2.4	$1,108$	$=0.12$
$80-90$	0.05	$1,405$	$=0.82$
$90-100$	2.4	$1,642$	$=0.12$
$100-110$	0.3	$1,244$	$=0.58$

Table 2.3: ANOVA of Effect of Lighting Conditions

Effect of Traffic Conditions

Rush hour usually means heavy traffic, especially for areas near downtown. Therefore, the effect of the rush hour on car-following behavior was investigated. The results are shown in Figure 2-8. It seems that except for the speed range 40-50 km/hr, there was no significant difference in the following distance under these two different conditions. An ANOVA was computed on the cell means. Table 2.4 shows the results and confirms this observation. It appears that rush hour has little effect on drivers car-following behavior.

$SpeedRange(km/h)$	F	$d.f$	P
$30-40$	0.57	$1,709$	$=0.45$
$40-50$	6.24	$1,222$	$=0.013$
$50-60$	0.12	$1,89$	$=0.73$

Table 2.4: ANOVA of Effect of Rush Hour

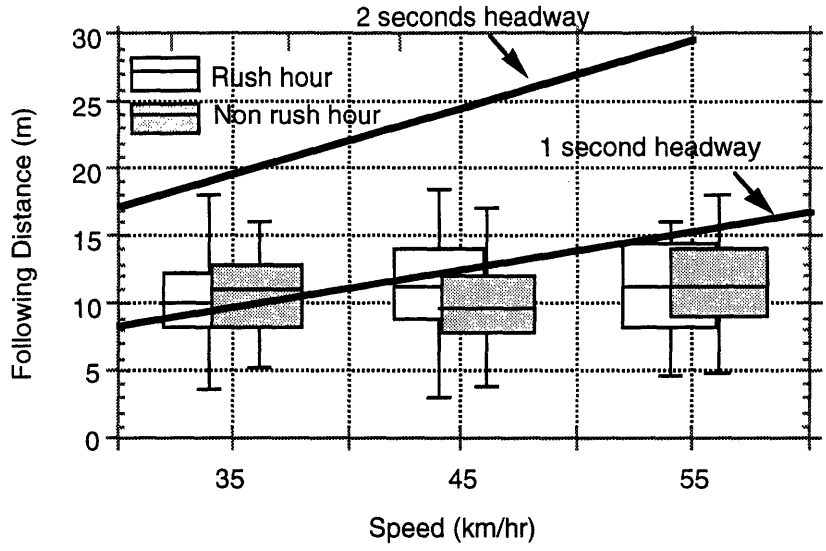

Figure 2-8: Comparison of Following Distance during Rush and Non-rush Hour

Effect of Location

Figure 2-9 compares the nighttime data from the two different locations. Overall, the average nighttime following distance on I-93 was approximately 15 percent greater than that on I-90. The ANOVA in Table 2.5 shows that the difference was significant at ranges from 70 to 90 km/hr but not at the range 90 to 100 km/hr. The cause of this difference may be the fact that there are 4 lanes on I-90 while only three lanes on I-93. Also, the existence of a downstream exit on I-93 from where we took the data, compared to no exit for about 2 miles on that I-90 section, may also contribute to the difference.

$SpeedRange(km/h)$	F	$d.f$	P
$70-80$	16.33	$1,156$	< 0.001
$80-90$	16.23	$1,334$	< 0.001
$90-100$	1.	$1,341$	$= 0.32$

Table 2.5: ANOVA of Effect of Location

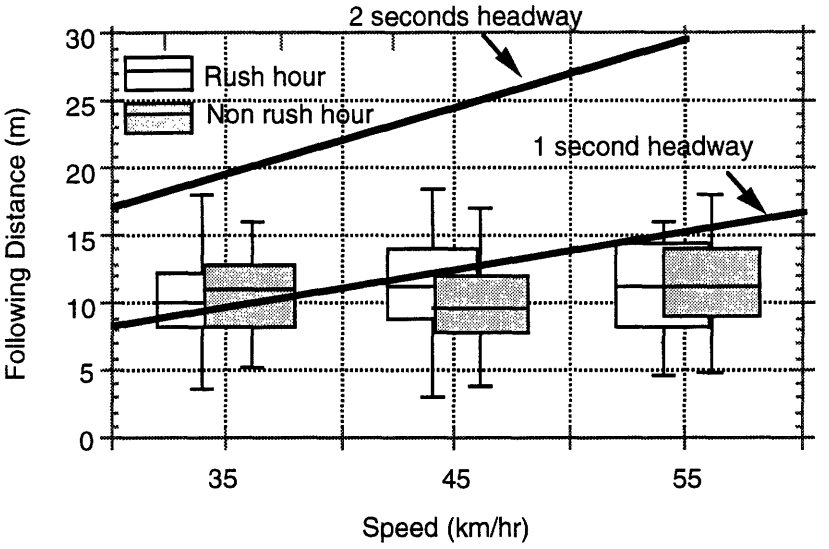

Figure 2-9: Comparison of Following Distance for Different Locations

Overall, the environmental effect of pavement wetness and illumination on driver car-following behavior seems to be minimal when the traffic is in free flow, while the effect appears to increase when the traffic becomes congested. As for traffic density, no obvious effect is shown for the collected data.

2.5 Summary

The video camera together with the stop-frame method provides a simple, yet accurate, way to measure car-following distance on the highway. The findings of the environmental effects on car-following behavior show some interesting results:

1. The speed-spacing relationship seems to be comprised of two separate regions, a "dual mode" behavior. The boundary of these two regions lies around a speed of 40-50 km/hr.

2. There is great variation among drivers in car-following behavior.

3. There is greater variation of following distance between drivers within a speed range than there is of means between speed ranges.

4. The environmental effect of pavement wetness and illumination on driver car-following behavior seems to be minimal when the traffic is in free flow, while the effect appears to increase when the traffic becomes congested. As for traffic density, no obvious effect is shown for the collected data.

5. Drivers in this study seem to keep the following distance well below the recommended 2 seconds headway.

Chapter 3

Simulator Tests

In most cases, the rationale for developing a driving simulator is to provide a safe and economical means for presenting an operational scenario in a controlled environment with readily available measures of system performance. Many examples of the acceptance and utilization of driving research simulators now exist throughout the United States, Europe and Japan. [16] [17] [18] [19]

3.1 Human-Machine Systems Laboratory (HMSL) Driving Simulator

The driving simulator developed in the Human-Machine Systems Laboratory provides a variety of possible parameter variations. Figure 3-1 shows the configuration of the simulator. The fixed-base car cabin allows the driver to control the vehicle through the existing gas pedal, brake, and steering wheel. Two audio speakers are used to

generate the sound environment. Steering wheel torque feedback is generated by a computer-controlled DC motor on the steering shaft. The motion of the vehicle is fed back to the driver mainly by the visual cues from the projection screen and secondarily by the feel of the steering wheel and the auditory cues which include engine noise (a function of speed) and a car-passing sound (change in loudness and pitch according to the closing speed and distance relative to on-coming cars). The road scene consists of a two-lane highway with vehicles in each lane. The subject's vehicle can pass or be passed by other vehicles. The detailed description of this simulator is in Appendix A.

Generally speaking, skilled drivers were able to sense the lateral acceleration through visual cues and steering wheel torque. This simulator has been tested and performance on it compared to results from actual road test with regard to longitudinal distance to objects (there is tendency to keep a slightly larger distance in the simulator), oversteer on sharp curves (one tends to oversteer in the simulator because acceleration cues are missing), and other variables.

3.2 Experimental Tasks

The simulator was used to test the effect of driver experience, gender and intention to pass on car-following behavior, and to test the driver's braking reaction time under different conditions, such as lead car applying full brake and a suddenly appearing obstacle. In other words, car-following distance distribution and reaction time distribution under different driving conditions and under different speeds were measured using the HMSL simulator.

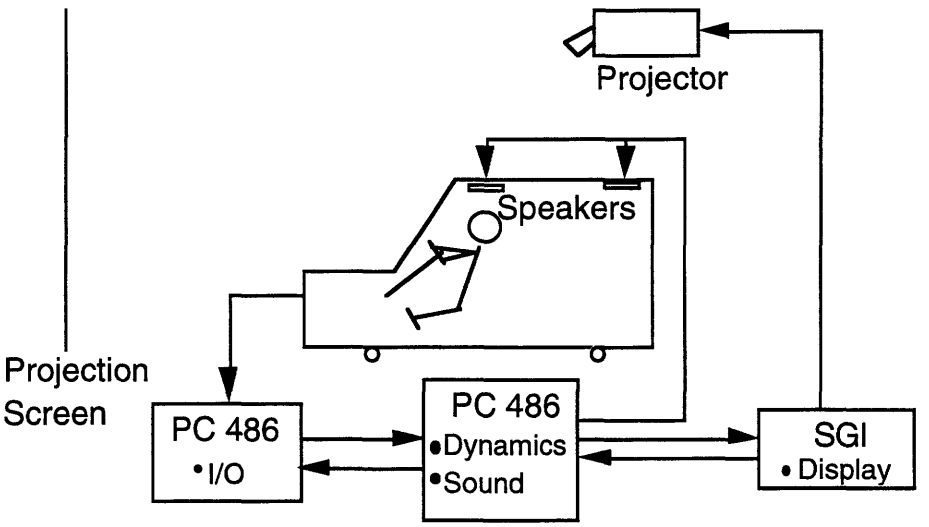

Figure 3-1: Configuration of HMSL Driving Simulator

The subjects were first given oral and written instruction describing the task and the procedure of the experiment. They were then given practice driving the simulator for as long as necessary in order to easily handle the vehicle and be familiar with a variety of presented scenarios that would appear in later experiments (usually 15 minutes). Immediately following the practice, two different experiments were conducted with about 12 minutes for each experiment and a 5-minute break between them. In the first experiment, the subjects were instructed to follow the lead car and to change speed or to brake as they would in normal driving according to the lead car conditions. The lead car changed speed randomly and occasionally braked to stop. For the second experiment, the subjects were asked to drive at their normal speeds and were allowed to pass whenever possible without collision. There were "no passing" zones and on-coming cars to limit the passing frequency. Following distances at different speeds were continuously recorded in the computer, and braking reaction

times were measured whenever the lead car applied its brake. This reaction time was measured from the onset of the lead car braking until the onset of the subject's applying maximum braking.

3.3 Subjects

The 35 drivers tested in the simulator were all holders of a current U.S. driver license. None of the drivers was professional. The subjects had been selected on the basis of their driving experience, age, and gender. The 11 senior subjects, with a mean age of 72, were all experienced drivers with more than 40 years of driving experience. The 24 young subjects included:

(1) Inexperienced drivers, with a mean of 1.3 years of driving (σ = 0.5 year), and a mean age of 27.2 (σ = 2.2).

(2) Experienced drivers, with a mean of 6.3 years of driving (σ = 1.8 years), and a mean age of 29.7 (σ = 5.5).

(3) Female drivers, with a mean of 3.8 years of driving (σ = 2.4 years) and a mean age of 29 (σ =5.2).

(4) Male drivers, with a mean of 4.0 years of driving (σ = 3.1 years) and mean age of 28.3 (σ = 4.1).

Categorization into two experience levels was made on the basis of statistical risk of accident, assuming drivers with up to 2 years experience have a higher risk of accident.

All subjects were volunteers and were not paid for their services during the period of approximately 1 hour required for testing.

3.4 Results

The log-normal distribution was assumed to compare the mean following distance for each experimental condition.

The main effect of driver experience on following distance was statistically significant (P<0.05) for all speed ranges except for the range of 60-70 km/h (P=0.34). The detailed ANOVA analysis is shown in table 3.1. Overall, the inexperienced drivers kept larger following distance than experienced drivers did.

$SpeedRange(km/h)$	F	$d.f$	P
$40-50$	50.37	$1,1000$	< 0.01
$50-60$	17.38	$1,1623$	< 0.01
$60-70$	0.8	$1,2221$	$= 0.34$
$70-80$	309.57	$1,2324$	< 0.01
$80-90$	136.13	$1,2230$	< 0.01
$90-100$	14.43	$1,2499$	< 0.01
$100-110$	12.45	$1,1780$	< 0.01
$110-120$	7.68	$1,1050$	< 0.01

Table 3.1: ANOVA of Effect of Driver Experience

Table 3.2 shows the ANOVA for different genders of drivers. Except for speed ranges of 40-50 and 100-110 km/hr, differences in the following behavior for male and female drivers were statistically significant. The average following distance for female drivers was larger than that for male drivers.

$SpeedRange(km/h)$	F	$d.f$	P
$40-50$	2.08	$1,1000$	$=0.15$
$50-60$	16.66	$1,1623$	<0.001
$60-70$	31.05	$1,2222$	<0.001
$70-80$	14.92	$1,2324$	<0.001
$80-90$	12.60	$1,2230$	<0.001
$90-100$	19.61	$1,2136$	<0.001
$100-110$	1.08	$1,1780$	$=0.30$
$110-120$	96.72	$1,1050$	<0.001

Table 3.2: ANOVA of Effect of Driver Gender

The driver intention to pass had great effect on following distance as shown in table 3.3. The data seemed to suggest that before passing, drivers slightly increased following distances.

$SpeedRange(km/h)$	F	$d.f$	P
$40-50$	58.97	$1,1000$	<0.01
$50-60$	1.36	$1,1623$	$=0.24$
$60-70$	36.01	$1,2222$	<0.01
$70-80$	9.52	$1,2324$	<0.01
$80-90$	217.87	$1,2230$	<0.01
$90-100$	382.63	$1,2136$	<0.01
$100-110$	382.74	$1,1780$	<0.01
$110-120$	40.43	$1,1050$	<0.01

Table 3.3: ANOVA of Effect of Driver Intention to Pass

The effect of age on car-following behavior is easily seen from the box plot. Figure 3-2 shows the detailed result. The effect was obviously statistically significant ($P<0.01$) for all speed ranges. The mean following distance for the senior drivers is almost twice that for the younger drivers.

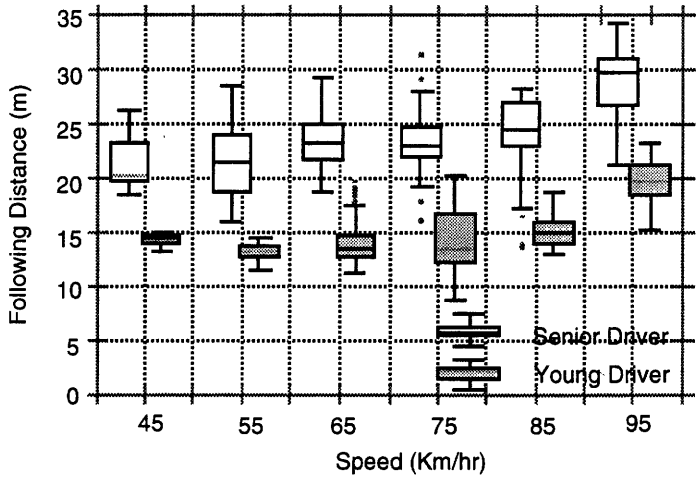

Figure 3-2: Comparison of Following Distance for Senior and Young Drivers

Figure 3-3, 3-4 and 3-5 show the box plots for following distances for different experience, gender and intention to pass. Using the same recommended following headway, i.e., 2 seconds, we can see that the following distances from the simulator test were well below the recommended distances.

Figure 3-6 shows the cumulative frequency function for braking reaction time for the young drivers. The mean reaction time for the lead car applying its emergency brake is 1.25 seconds, while that for sudden appearance of an obstacle is 1.10 seconds. Both reaction times include perception time and foot movement time. These results are very close to those from Olson's experiment under surprise conditions [23]. For the senior drivers, the distribution is shown in figure 3-7. The average reaction times

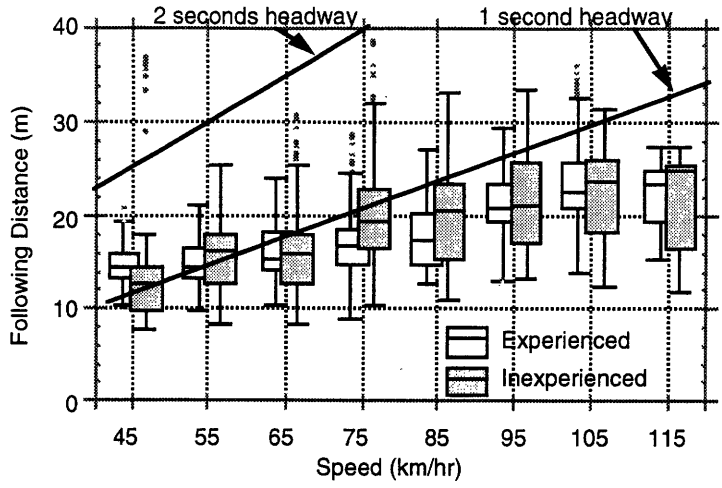

Figure 3-3: Comparison of Following Distance for Young Experienced and Inexperienced Drivers

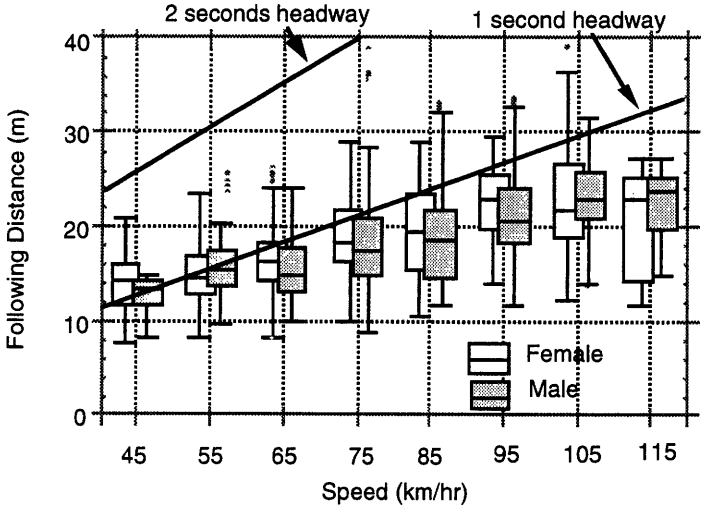

Figure 3-4: Comparison of Following Distance for Young Female and Male Drivers

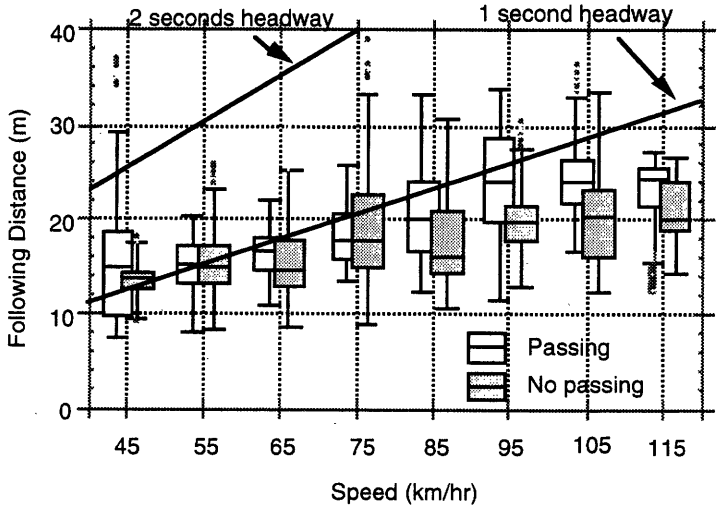

Figure 3-5: Comparison of Following Distance with Passing and No-passing

for emergency braking and sudden obstacle are 1.5 and 1.3 seconds, respectively. It is obvious that the reaction time increases with age. The difference lies in the longer perception time for the senior drivers than for the younger drivers.

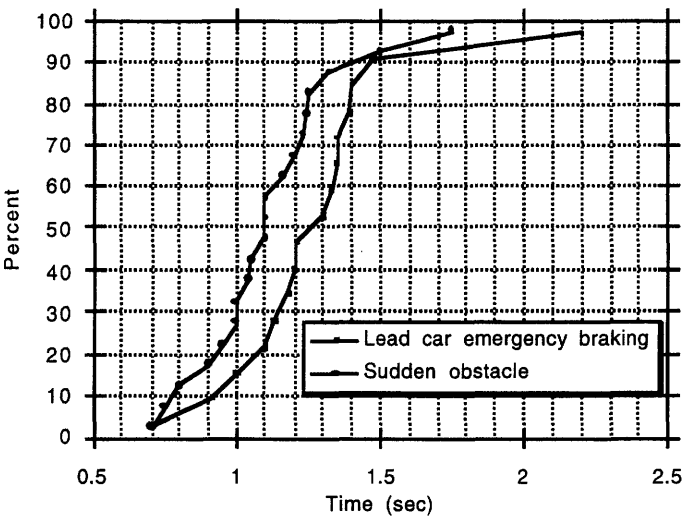

Figure 3-6: Braking Reaction Time for Young Drivers

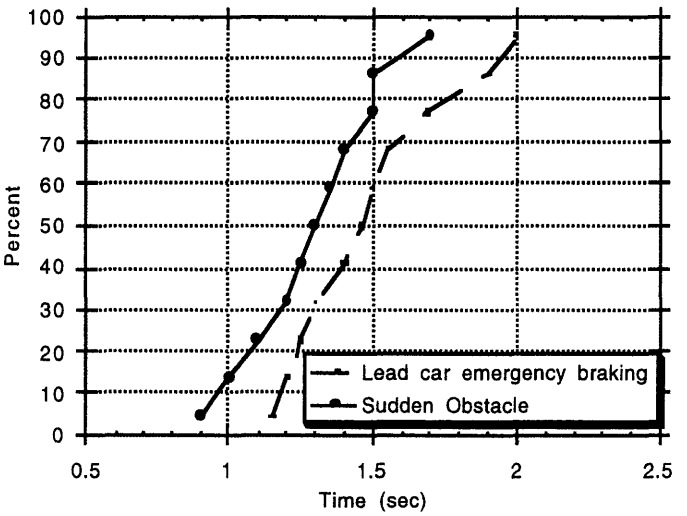

Figure 3-7: Braking Reaction Time for Senior Drivers

3.5 Summary

The HMSL driving simulator proved to be effective in the research of driver car-following behavior and braking reaction. The effects of driver characteristics on car-following behavior are statistically significant in terms of driver experience, gender, intention to pass and age. These results provide a guideline for designing a collision avoidance system that is intended to suit individual needs. The braking reaction time distribution is reasonable compared to other research, and thus will be used for the modeling purpose of the next chapter.

Chapter 4

An Integrated Method for Evaluating Car-following Safety

The car-following data discussed in the previous two chapters clearly shows that there might not be a simple mathematical form to represent car-following distance in a general way. Even if a more complex form can be found, it could be too complex for the car-following safety analysis. This chapter discusses a model developed to estimate safety. The model is called CARMASS which stands for **CAR**-following Model **A**nd **S**afety **S**imulation.

4.1 Framework of the Model

Figure 4-1 diagrams the framework for evaluating the safety of car-following. The car-following distance distribution is acquired using the data from highway measurements. The distribution of driver reaction time, on the other hand, comes from the results of

the simulator test only. The vehicle braking characteristics are dependent on vehicle type, vehicle speed, and road surface conditions. The discrete following distance and stopping distance are sampled separately using the Monte Carlo method, assuming these conditions are independent of one another. The difference between these two distances then forms the distribution of safety margin under that particular condition. The status of the interaction, collision or not, is then determined.

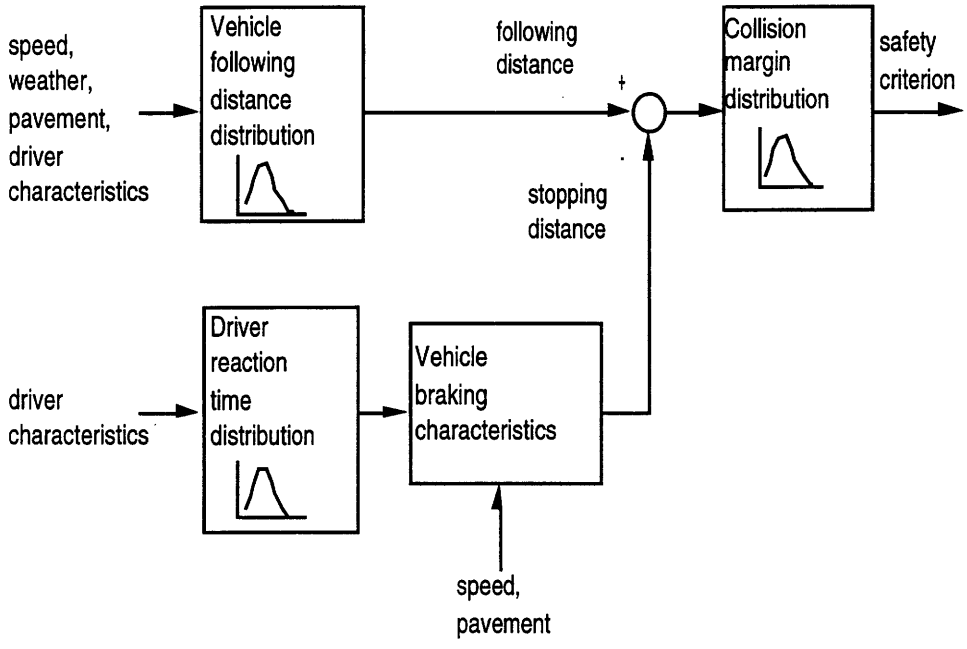

Figure 4-1: Block diagram of the car-following evaluation algorithm

The kinematics in determining the safety of car-following are straightforward if all the factors to be considered are available. The factors to be considered include variables from driver, environment and vehicle. A collision scenario means that a driver keeps too short a distance to react soon enough to stop his/her own vehicle

before reaching the lead car stopping position. Therefore, the car-following safety model compares the car-following distance (D_f) and the safe relative distance (D_s) between the two cars. If the difference is positive, there is no collision. Otherwise, there is a collision. Equation 4.1 shows this simple relation.

$$\Delta = D_f - D_s \tag{4.1}$$

where Δ = margin to collision, D_f = car-following distance, D_s = safe relative distance.

The car-following distance is obtained from the highway data while the safe relative distance makes use of the following equation:

$$D_s = V_f T_r + \frac{1}{2}[\frac{V_f^2}{\alpha_f} - \frac{V_l^2}{\alpha_l}] \tag{4.2}$$

where

D_s = the stopping distance required to avoid collision,

V_f = the speed of following car,

T_r = the driver braking reaction time,

V_l = the speed of lead car,

α_l = the deceleration of lead car,

α_f = the deceleration of following car.

The parameters α_f and α_l are dependent upon the assumed vehicle braking characteristics while T_r varies according to the probability distribution derived in chapter 3. For the extreme case of a sudden-stopped obstacle or vehicle moving perpendicu-

lar to own vehicle path, the effective α_l is infinity and the required stopping distance would be the largest.

The probability distribution of collision is obtained through the Monte-Carlo integration of the two distance distributions

$$P(\Delta < \delta) = \int P(D_s = x)P(D_f > \delta + x)dx \tag{4.3}$$

where

$P(\Delta < \delta)$ = the probability of margin to collision less than δ,

$P(D_s = x)$ = the probability of car-following distance equaling to x,

$P(D_f > \delta + x)$ = the probability for safe relative distance larger than $\delta+x$.

When $\delta = 0$, the result represents the probability of collision. For detailed discussion of the analytical model, see Appendix B.

4.2 The CARMASS Model

CARMASS is a quasi Monte-Carlo simulation which uses car-following data recorded from the real highway as a source of realistic information on vehicle speeds and following distances in traffic. The simulation also incorporates routines to represent the effect of the driver's reaction time and hence the potential for collisions. The objective is to develop a tool that can be used to (1) investigate the sensitivity of rear-end collisions to various kinematic parameters and assumptions, (2) provide some insight into the effectiveness and limit of potential intelligent cruise control.

4.2.1 Scenario

The model simulates the scenario for a lead vehicle and a following vehicle traveling in the same lane. At time T_0, the lead car applies emergency braking and slows to a stop. After some human response time delay, the driver of the following vehicle begins to brake if no automatic braking control is available, or the automatic braking control begins to brake after some sensor time delay. The parameters that determine whether or not a rear-end collision occurs are:

1. the lead vehicle's speed,
2. the following vehicle's speed,
3. the following distance,
4. the two vehicles' deceleration,
5. the reaction time of the following vehicle's driver to the onset of lead car braking, and
6. the reaction time of potential intelligent cruise controllers.

Following sections discuss the basis for specifying each of the these parameters.

4.2.2 Assumptions

Several assumptions were made to simplify the analysis process or to make the simulation more realistic.

Braking Reaction Time

Random values for the braking reaction time are obtained from the distribution described in chapter 3. As discussed before, this distribution was based on the surprise reaction time data with the following speed at around 55 km/hr. However, drivers may be more alert when keeping shorter following distances as suggested by Farber et al. [20]. Accordingly, the reaction time for alert drivers should be shorter than for non alert drivers. Based on Johansson et al. study [21], the correction factor for surprise and alert reaction time is about 1.3. This will be adopted in this thesis as an assumption in order to make the simulation more realistic.

Lead Car Deceleration Level

For an emergency situation, it is assumed that the driver of the lead vehicle will brake at or near the limit of tire-pavement friction. Hence the braking level for the lead car under investigation is fixed at 0.7g or $6.86 m^2/s$, a level achievable on dry pavement by vehicles capable of meeting FMVSS 105, the Federal Motor Vehicle Safety Standard for braking. Since about 80% of rear-end crashes occur during dry weather, only dry weather is under consideration for this model [22].

Following Car Deceleration Level

It is again assumed that, in an emergency, the following driver will apply full brake as described for the lead car braking limit. For an automatic braking-control vehicle, the

deceleration level is set to the desired level for the controller. To maintain deceleration at a comfortable level, the braking is limited to $2.5m^2/s$.

4.2.3 Structure

As noted above, CARMASS is a quasi Monte-Carlo simulation. Vehicle speed and following distance and driver's braking reaction time are random variables, sampled from appropriate distributions discussed in previous two chapters. The lead vehicle's braking level is set at emergency braking. The following vehicle's braking level depends on whether or not an automatic braking control is used.

In each single iteration of the model, the following speed and distance of a vehicle are read from the traffic data file. Random values are drawn from the following driver's braking reaction time for manual control. CARMASS then calculates, given these initial conditions, the margin to collision based on the kinematics explained in the previous sections.

4.3 Simulation Results

To illustrate the procedure, consider the following four examples for different control actions. The distribution of the car-following distance under daylight and dry pavement acquired from the highway data, as shown in Figure 4-2, are used for all the examples.

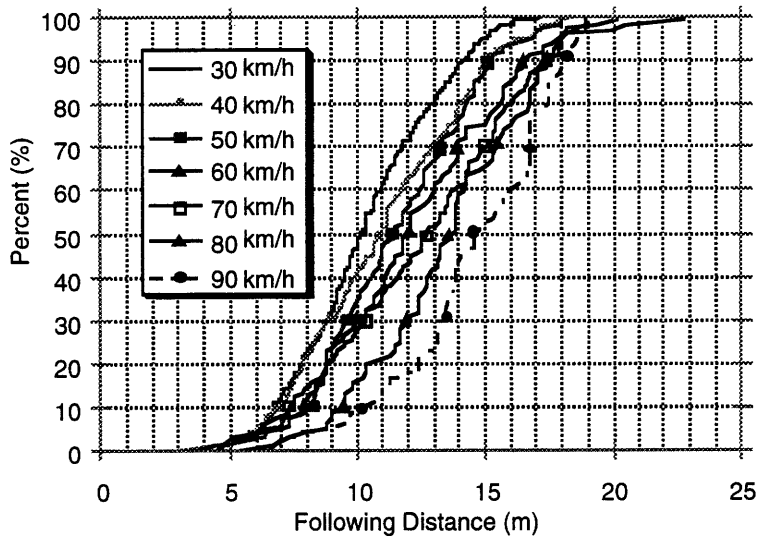

Figure 4-2: Cumulative frequency distributions for car-following distance

4.3.1 Manual Control

The first example considers the driver response when the lead car suddenly brakes fully to stop and there is no automatic braking control. The distribution of the brake reaction time is described in figure 3-6 for this special case. The stopping distance for this special case was derived by using equation 4.2. Using the Monte Carlo sampling method, the safety margin is a distribution as shown in figure 4-3. From this hypothetical result one can see that under this special condition, most of the population will have a collision for all the speed ranges. Note that in this example, the braking reaction time is based on a "surprise" reaction time. Figure 4-4 shows the result when the following drivers are in an alert condition and thus the braking reaction time is reduced by a factor of 1.35. There is slight improvement in terms of margin-to-collision; however, the majority of the drivers still have a collision.

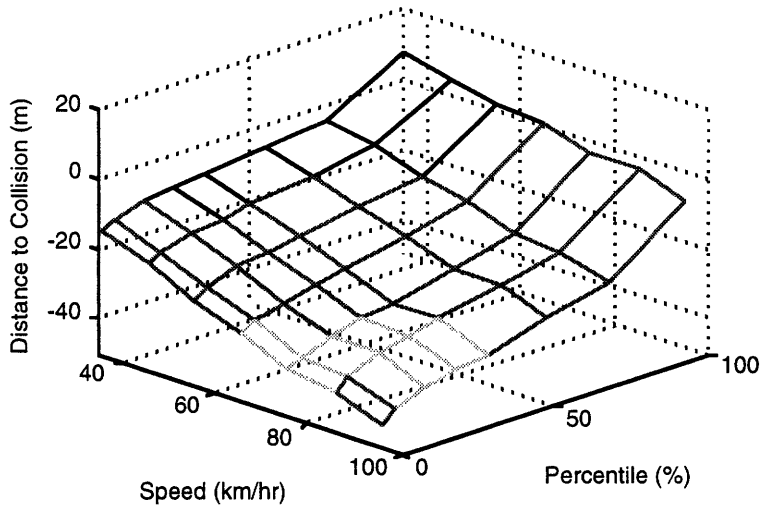

Figure 4-3: Hypothetical distribution of the safety margin with lead vehicle emergency braking, without any braking control and with a "surprise" reaction time

4.3.2 Engine Control

The second example involves the case when the lead car applies full braking, and automatic engine braking control is applied to the following vehicle. In this case, the driver reaction time is replaced by the sensor/actuator delay time, assumed to be 0.3 second. The engine braking characteristics varies for different vehicles. An

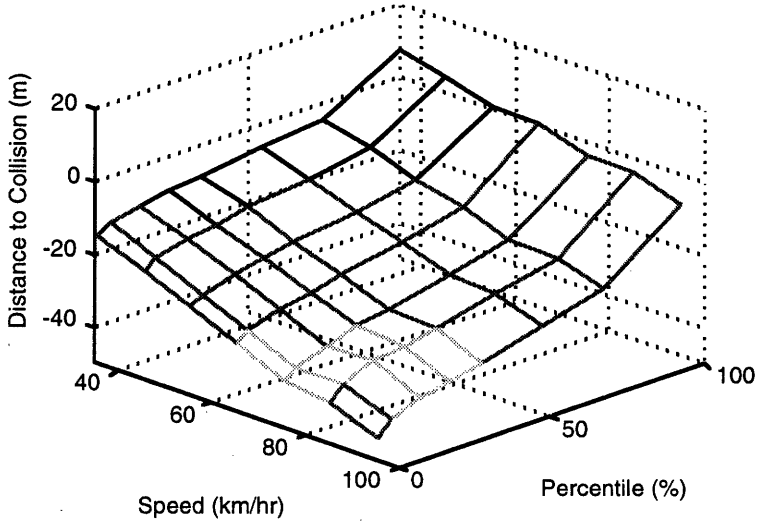

Figure 4-4: Hypothetical distribution of the safety margin with lead vehicle emergency braking, without any braking control and with alert reaction time

approximate equation has a first order response

$$Deceleration(t) = A * (1 - e^{B}) \tag{4.4}$$

where A and B are two constants.

Due to lack of detailed data for engine braking, we ignore the fact that the deceleration rate should change according to the gear ratio and the vehicle speed and assume the rate to be constant. Figure 4-5 shows the hypothetical result. It is clear that with automatic engine braking the outcome is worse than for manual braking since the deceleration rate is very small for engine braking compared to that for regular braking. Therefore, it is reasonable to conclude that engine braking can only be used to slow the vehicle under normal conditions rather than to stop the vehicle in an emergency situation like the one assumed in this example.

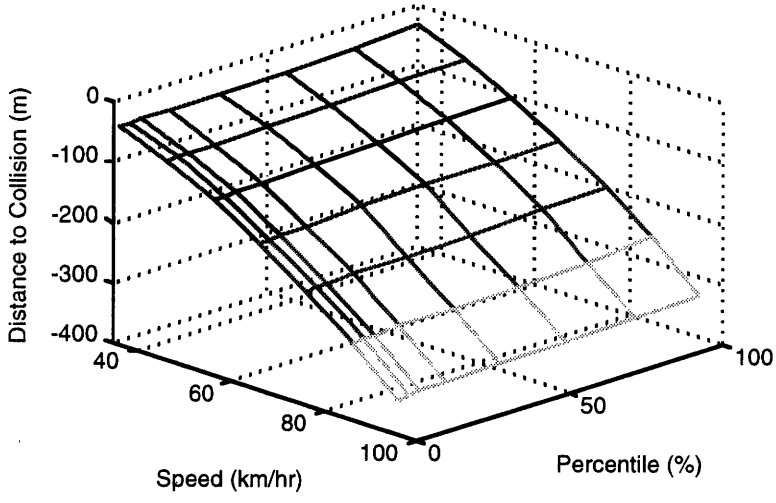

Figure 4-5: Hypothetical distribution of the safety margin with lead vehicle emergency braking and with automatic engine braking control

4.3.3 Limited Automatic Braking Control

The third example shows the case where the lead car applies emergency braking and an automatic braking control is activated. However, in order for the vehicle to be operated at a comfortable maneuvering level, the deceleration rate is limited to $2.5m/s^2$. The sensor/actuator delay is again assumed to be 0.3 second. Figure 4-6 shows the simulation results. One can see that with this limited braking, collision can only be avoided for a very small population and only for low speed conditions.

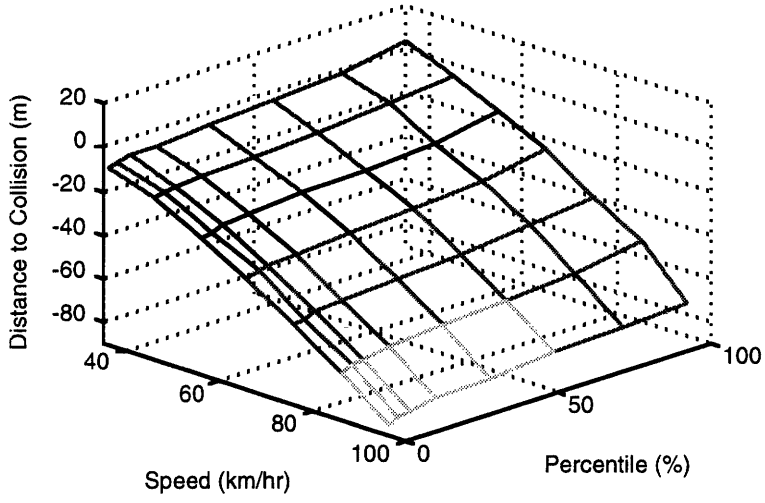

Figure 4-6: Hypothetical distribution of the safety margin with lead vehicle emergency braking and with limited automatic braking control

4.3.4 Full Automatic Braking Control

For the last example, assume maximum deceleration is allowed for the automatic braking control. Obviously, the result will be much better than that for limited braking. Figure 4-7 shows that most of the population will avoid collision under this condition.

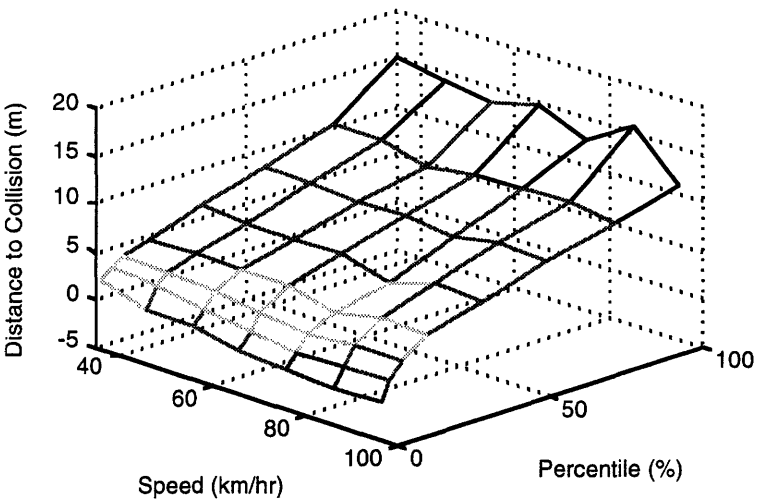

Figure 4-7: Hypothetical distribution of the safety margin with lead vehicle emergency braking and with full automatic braking control

4.4 Correction Factors

The procedure can be modified with some correction factors for different assumed conditions but using similar statistical distributions. For example, data from the highway measurements show there is 0.9 meter greater average following distance under wet road surface for speed range 30-40 km/h. The safety margin might then be estimated by simply shifting the distribution of safety margin to the right by 0.9 meter. In this case the collision probability would be 94% instead of 96% as in the dry surface condition (assuming the reaction time remains the same). Figure 4-8 shows this hypothetical shift.

The procedure can be further refined to include correlation at the stage of Monte Carlo sampling between reaction times and following distances (a young man with faster reaction times follows more closely) and of course can be improved upon with better data as it becomes available.

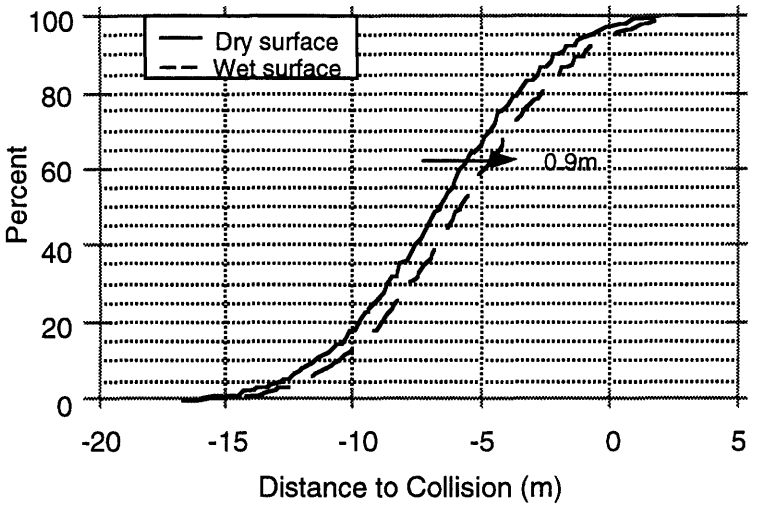

Figure 4-8: Hypothetical shift of distribution of the safety margin for dry and wet road surface

4.5 Summary

Although CARMASS incorporates many simplifying and idealizing assumptions, it provides a simple way to estimate car-following safety. It is important to keep in mind that the findings reflect these assumptions and only provide "potential" collision. The high frequency of collision resulting from long braking reaction time seems unrealistic and of course our examples are based on the most extreme and worst-case assumption of lead-car behavior. However, even with moderate reaction times, drivers still are driving in a risky situation. This can be seen from the very short headway that drivers keep when they are following a lead car. Though significant rear-end collisions are a rare event for a given driver, it is the designer's responsibility to understand any potential risks and design a device that can help drivers avoid these rare events. Simulation results from CARMASS can provide a guideline for designing and evaluating such a device. It is shown that engine braking control may not be used for the

purpose of avoiding collision. Such limited braking can avoid collision only if drivers are willing to give up short following distance. Full braking is the only option if the driver's desire of following closely is to be satisfied.

Chapter 5

Demonstration of Intelligent Cruise Control

The results from chapter 4 indicate potential collisions in car-following if the emergency scenario does occur. Many reports have indicated that the major contributing causes of the discussed accident scenario are driver inattention (long reaction time) and following too closely (small headway) [24] [25]. Since we may not be able to change driving habits, it is evident that the only way to help drivers avoid collisions in emergency is to reduce driver reaction time. This can be done either by using a warning system which will arouse the driver's attention or by employing intelligent cruise control which will detect an emergency situation and respond with a delay which only a fraction of the driver reaction time .

Intelligent cruise control is a system designed to control relative speed and distance between two consecutive vehicles in the same lane. An ICC system can be consid-

ered as an extension of the traditional cruise control. Over the past few decades, ICC researchers have been focusing on developing more reliable sensors and image processing technology [6] [10] [13]. Some important, non-technical issues that will affect the success of ICC are yet to be resolved. Among them, how to make a proper trade-off among comfort, convenience and safety is a question frequently asked by human factors researchers. In another words, whether ICC can provide support to suit each individual need is our main concern. A successful ICC needs not only to deal with the complex driving task in the presence of hard disturbances such as appearance of obstacles, but it also must have the capability of imitating driver car-following behavior. This chapter describes the design of a fuzzy-logic based ICC which utilizes the car- following model derived in the previous chapter and provides on-line learning process to mimic the driving behavior without much sacrificing safety and comfort.

5.1 Overview of Proposed ICC System

The overall vehicle system equipped with the proposed ICC is shown in figure 5-1. There are three blocks or modules in this diagram. The fuzzy control block is the main part of the ICC and will be discussed in more detail in the next section. The vehicle block denotes the vehicle's equipment and its interaction with the ICC and the environment. The speed control block stands for the traditional cruise control that is usually included as a part of the ICC.

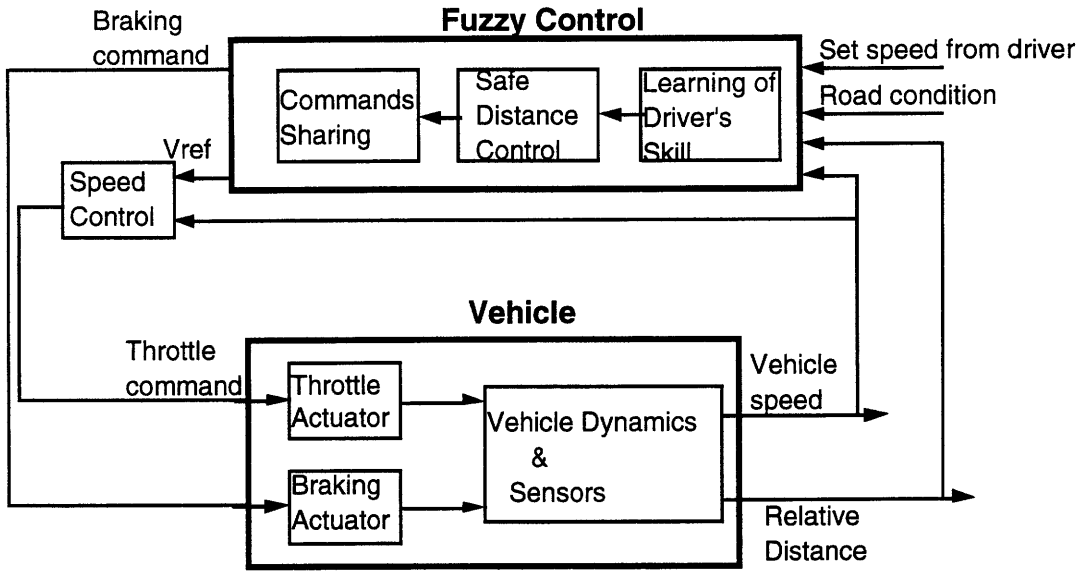

Figure 5-1: Vehicle System with ICC

5.2 Fuzzy-logic ICC

5.2.1 Fuzzy Set Application

Generally speaking, a good control theoretic design must be based on thorough knowledge of the system to be controlled, the environmental influences, and the relevant task elements. In many situation however, the structure of the system is unknown, parameter variation is unpredictable, or goals and constraints are not readily quantifiable by a single number. Fuzzy set theory, introduced by L.A. Zadeh thirty years ago [26], may be invoked to deal with such control problems. In fact, fuzzy set theory enables the conversion of linguistic control strategy, based on expert knowledge, into an automatic control strategy. The resulting algorithm usually preserves, or is marked by, the expert's subjective, inaccurate, incomplete, and maybe even contradictory

behavior.

Fuzzy set theory has a short yet remarkably rich history in process control and decision making [27]. For control of a number of ill-defined processes in particular, fuzzy-logic controllers have proven to be the most satisfying substitute for a skilled human operator. One of the first, and most striking, examples of fuzzy logic control is the control of a cement kiln by Holmblad and Ostergaard [28]. A brief introduction to fuzzy set theory is given in Appendix C.

Intelligent cruise control systems are based on the availability of fairly accurate measurements whereas most aspects of driver car-following behavior are much more inexact by nature. The non linearity of the vehicle dynamics and the uncertainty surrounding the environment and the driver further remove the classical linear control from consideration. In dealing with non-linearity and uncertainty, fuzzy set theory has been demonstrated to have design advantages over other non-linear control theories [29]. Thus, the proposed ICC system employs the fuzzy-logic technique in solving this complex control problem.

5.2.2 Safe Distance Control

As shown in figure 5-1, safe distance control is one of the major control elements of the ICC. The purpose of this module is to create a car-following criterion for the controller based on the results of the safety evaluation described in chapter 4. For example, if the control objective is to maintain a safe distance in all instances, and the control constraint limits the braking level to $2.5m/s^2$ (these two elements are adopted

by virtually all the ICC's currently been developed), the margin to collision from the simulation shown in figure 4-6 will be used to calculate safe following distances. Figure 5-2 shows the same graph in a 2-D form. If the overall ICC goal is to avoid collisions in an emergency, this goal can not be achieved without sacrificing the driver's desire of keeping a close following distance. Instead, the safe following distance for this special case would approximately increase to the distribution shown in figure 5-3 at a 95% level. The large increase of following distance is due to the use of limited braking for the sake of comfort. Again, this is a result of trading driver desire of following closely for the safety and comfort of driving. However, if the maximum braking capacity is allowed, the safe following distance will substantially decrease, perhaps to what the driver originally desires. Notice that this only provides the initial safe following distance distribution used for the ICC. Subsequently, the control module will modify the following criterion according to on-line learning of individual driver following behavior. This on-line learning is discussed in more detail in the following section.

5.2.3 On-line Learning of Driver Skill

One advantage of using fuzzy-logic for control design is to mimic the operator control action. In addition to incorporating the real-world driver following behavior into the design process, it is easy to implement the on-line learning of each individual driving habit. As shown in the previous section, the ICC trades the individual desire of following closely with overall safety and comfort. Unfortunately, this design may not appeal to some drivers who are either risk-prone or are willing to sacrifice some

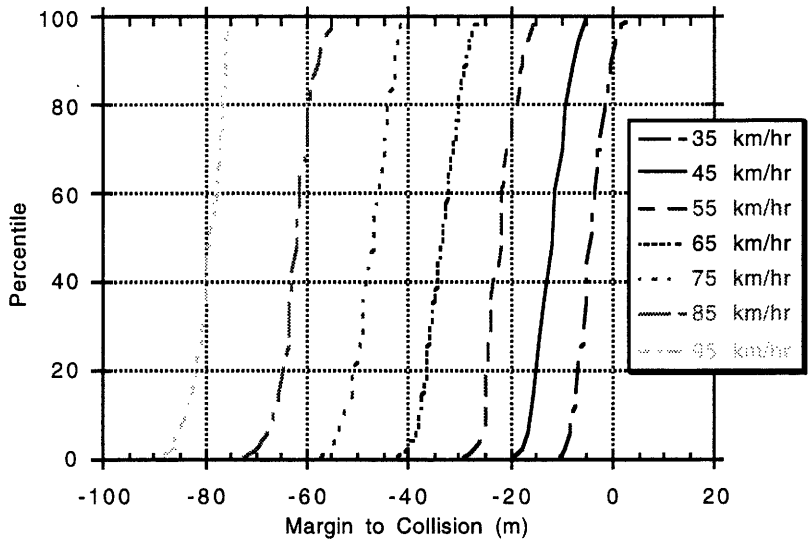

Figure 5-2: Margin to Collision for Limited Braking Control

comfort. The ICC can learn from observing driving action under different conditions while the ICC is disabled. For instance, the ICC could detect that the driver frequently brakes near maximum braking capacity. It then modifies the safe following control module to adopt a different safe following policy. Figure 5-4 shows the example when full braking is allowed. Note that the safe following distance is close to the observed driver following distance. This implies that if the observed following distance distribution reflects what drivers really like to maintain, the ICC must use full braking when emergency occurs in order to maintain safety.

5.2.4 Design of Fuzzy-logic ICC

For this application, the original form given by Mamdani is used for design of the fuzzy-logic ICC [30]. Mamdani's fuzzy control method can be characterized by a

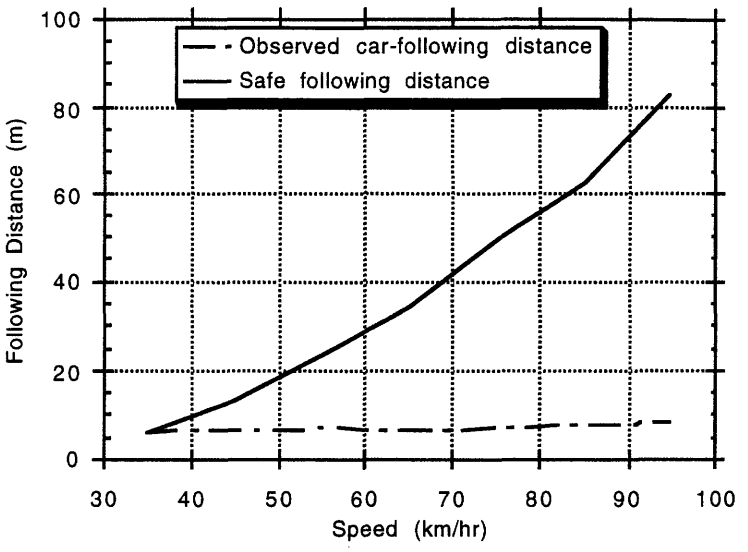

Figure 5-3: Safe Following Distance for the ICC

crisp relation and a context depending on the fuzzy equality. Vague rules are used to described characteristics of the system and commonly have the following form:

$$\begin{array}{lll} IF & \textit{absolute speed} \;\; IS \;\; \textit{fast} & AND \;\; \textit{distance} \;\; IS \;\; \textit{large} \\ AND & \textit{lead car} \;\; IS \;\; \textit{opening} & \\ \hline THEN & \textit{increase engine power slightly.} & \end{array} \tag{5.1}$$

Now the problem is to generate all the proper control rules in the if-then-else form for the overall controller. For demonstration purpose, the author simply tried out different possible driving rules based on some common sense. If the system involved becomes very large and complex, other procedures have to be taken to acquire the rules.

The detailed description of this fuzzy-logic controller is in Appendix D.

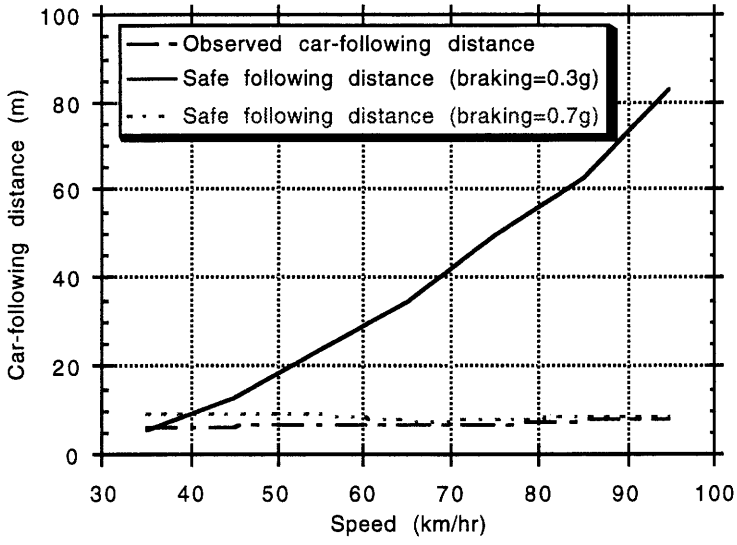

Figure 5-4: Safe Following Distance for the ICC after On-line Learning

5.3 Simulation Results

Three separate simulations were carried out to validate the controller design. For all three examples, the braking was limited to comfortable level of $2.5m/s^2$.

The first simulation, as shown in figure 5-5, involved the scenario that an ICC-equiped car was traveling at 80 km/hr and wished to maintain this speed. A slower car appeared at far distance and was approaching fast. When the distance reduced to near the safety limit, the ICC began to act by reducing engine output and eventually by applying the brake to slow down the car. Finally, the speed reduced to the same speed as the lead car and followed the lead car at constant distance. Note that the final following distance was maintained at about 20 meters, which represented the necessary condition for this particular ICC that was operating with limited braking.

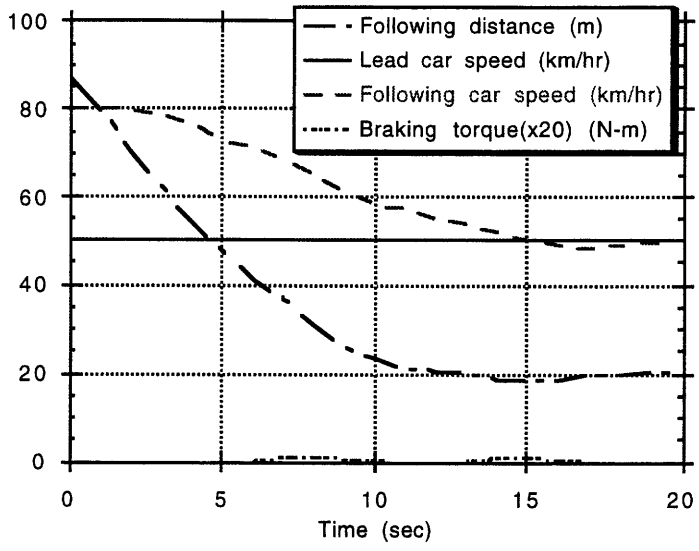

Figure 5-5: Example of Car-following with Lead Car Slow down

The second example simulated the case where sometime after the first scenario, the lead car sped up quickly to 90 km/hr. The ICC car reacted by increasing the speed back to 80 km/hr as set by the driver and maintained at that speed thereafter. The result is shown in figure 5-6. Note that in this case, the braking was never used and the following distance kept growing since there was a 10 km/hr positive relative velocity between the two vehicles.

The final example involved the scenario that after traveling at 80km/hr for some time, a slower car (traveling at 70 km/hr) appeared. At time t=4 second, the lead car applied emergency braking. The ICC reacted by applying maximum braking allowed, i.e., $2.5m^2$, to stop the car to avoid collision. Note that the final distance between the two stopping cars was about 3 meters. Therefore, a potential collision was avoided.

These three simulation results show that the fuzzy controller can perform both

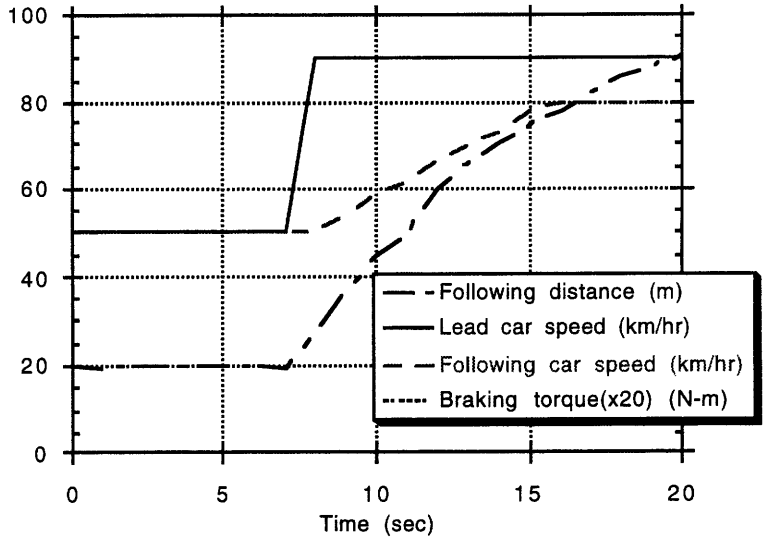

Figure 5-6: Example of Car-following with Lead Car Speed up

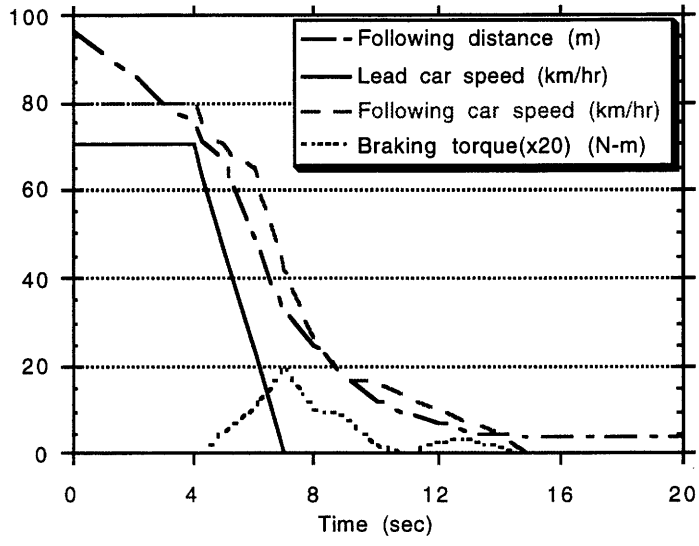

Figure 5-7: Example of Car-following with Lead Car Emergency Stop

speed and distance control under different conditions. Note that a low-pass filter was added to the fuzzy-logic controller to smooth out the control output for all three cases.

5.4 Summary

The design process for a fuzzy-logic intelligent cruise controller based on the results from the CARMASS was demonstrated in this chapter. Using fuzzy-logic evidently helps realize the complete control system in a very short period of time and avoids complicated mathematical analysis.

The ICC can assist drivers, with observed car-following behavior, in avoiding collisions in an emergency only when the ICC is using full braking capacity. In the case that comfort is the main concern, the ICC must increase the safe distance to an extent that some drivers may not like to have the ICC. The trade-off problem may be resolved through on-line learning.

Some simulation examples were shown to validate the ICC. The results showed that the ICC successfully performed safe car-following and collision avoidance.

Chapter 6

Conclusions and Recommendations

6.1 Conclusions

A driving simulator was first designed for the purpose of carrying out car-following research in the laboratory. This simulator provides most of the necessary elements to achieve realistic driving, including sound environment, force feedback on the driving apparatus and realistic visual environment. Numerous experiments carried out on this simulator proved its adequacy and effectiveness.

Understanding Driver car-following behavior is important in the design of any driver aid. While a lot of research has been focused on a mathematical model of car-following in overall traffic flow, very little has been done regarding individual car-following behavior in a steady traffic stream. This thesis investigates the driver's

car-following behavior in a steady traffic stream on both actual highways and in a simulator creates a data base that can provide for future research in related areas.

The study of car-following behavior reveals following important information:

1. The speed-spacing relationship seems to be comprised of two separate regions, a "dual mode" behavior. The boundary of these two regions lies around speed of 50 km/hr.

2. There is great variation among drivers in car-following behavior, and no simple function relating following distances to vehicle speed as appropriate.

3. There is greater variation of following distance between drivers within a speed range than there is between speed ranges.

4. The environmental effect of pavement wetness and illumination on driver car-following behavior seems to be minimal when the traffic is in free flow, while the effect appears to increase when the traffic turns into congested flow. As for traffic density, no obvious effect is shown for the collected data.

5. Drivers in Boston area seem to keep the following headway well below the 2 seconds recommendation value.

6. The effects of driver characteristics on car-following behavior are significant. General speaking, male drivers keep smaller distance than female drivers , experienced drivers keep smaller distance than inexperienced drivers, and younger drivers keep smaller distance than older drivers. smaller distance.

This thesis also investigates driver braking reaction time in a simulator under different assumptions. The results show that while older drivers do have longer reaction times, experience and gender seem to have little effect on overall reaction time. The mean values vary from 1.1 seconds to 1.5 seconds for response to lead car using emergency braking.

Using the experimental data of car-following and braking reaction time, a numerical model for estimating car-following safety is proposed and some examples are given to demonstrate its feasibility. The simulation results show potential car-following safety problems when drivers are responsible for unexpected emergency traffic conditions. On the other hand, intelligent cruise control system shows its potential in helping drivers by reducing reaction time.

Based on the CARMASS simulation results of safety, a simple fuzzy-logic intelligent cruise controller is developed. The controller can perform basic speed control as well as more sophisticated safe distance control. It also has an ability to learn individual driver's habits provided they are within the preset safety limit. A simulation result shows the effectiveness of this controller.

6.2 Direction for Future Research

While a data base for steady car-following has been established, it is never a complete work. More data must be taken and analyzed to really understand the interdependency of all the environmental factors. A multiple regression model is worthy

of exploring when additional data become available.

Although the comparison of car-following behavior as a function of driver characteristics has been made with the HMSL driving simulator, the following data still are not comparable to real highway data. A more detailed calibration of the HMSL driving simulator is necessary to generalize measured behavior on the control highway.

The CARMASS model presented here assumes that the deceleration levels for both the lead car and the following car are identical for the simulation. Consideration of the difference between these two needs to be explored. This approach will lead to a more general car-following model.

The intelligent cruise control designed in this thesis provides a simple example of utilizing the safety margin as a basis for design. The controller has been shown to be effective in performing classical speed and safe distance control tasks. However, the adaptiveness, or the learning ability, of the controller needs validation.

Appendix A

HMSL Driving Simulator

A.1 Overview

The objective of the HMSL simulator is to provide a basic tool for driver-related research with acceptable simulator fidelity. The general block diagram for the HMSL driving simulator is illustrated in figure 3-1 and is redrawed here in figure A-1. The whole simulator is under control of the host PC-486 computer, which directs the scenario or event sequence encountered by the driver. An instrumented cab is tied in with this host computer and another PC-486 computer and some subsidiary electronic equipment are arranged to provide interactive steering and speed control for the driver. Control signals from the cab are processed by the host computer using vehicle equations of motion to yield vehicle motion commands for the main visual display system, instrument drive signals (speedometer), auditory display (engine and road noise, tire squeal, crashing, wind, etc.), and other subsidiary visual display (rearview

scenes).

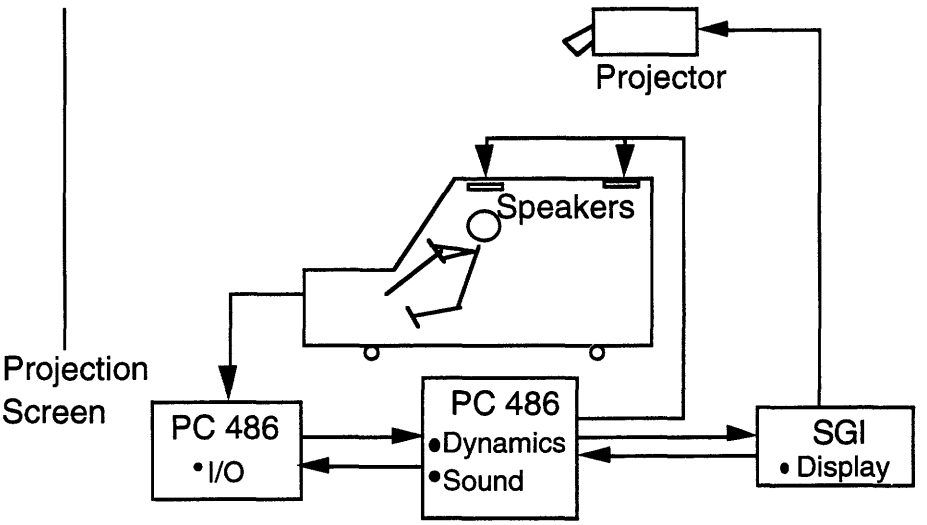

Figure A-1: Configuration of HMSL Driving Simulator

A.2 Functional Components

A.2.1 Visual Display

Visual inputs provide the predominant cues for driving. The delineated path to be followed must be perceived visually, along with other vehicles or obstacles that must be avoided. The resolution of these cues is not usually critical to steering and speed control tasks but is crucial to distance control. The driver controls the vehicle's path through combined perception of heading angle and lateral position relative to the commanded path, and the local curvature of the commanded path [31]. Smooth motion of the commanded path display is an important factor because image textural

"streaming" across the retinal field is an important cue for vehicular control [32].

With these design requirements, a good visual display generator is needed even for a low-cost, fixed- base simulator such as the one designed here. A SiliconGraphics Indigo-II Extreme is used to generate high resolution graphics and a Barco-800 projector is used to project the image on a large projection screen sized 12'x8'. The screen refresh rate is about 20 frames/sec which is at the lower limit of smooth motion. This updated rate, however, is slightly lower than the recommended 0.04 second computation delay [33].

A general scene seen by the driver from the cab is shown in figure A-2

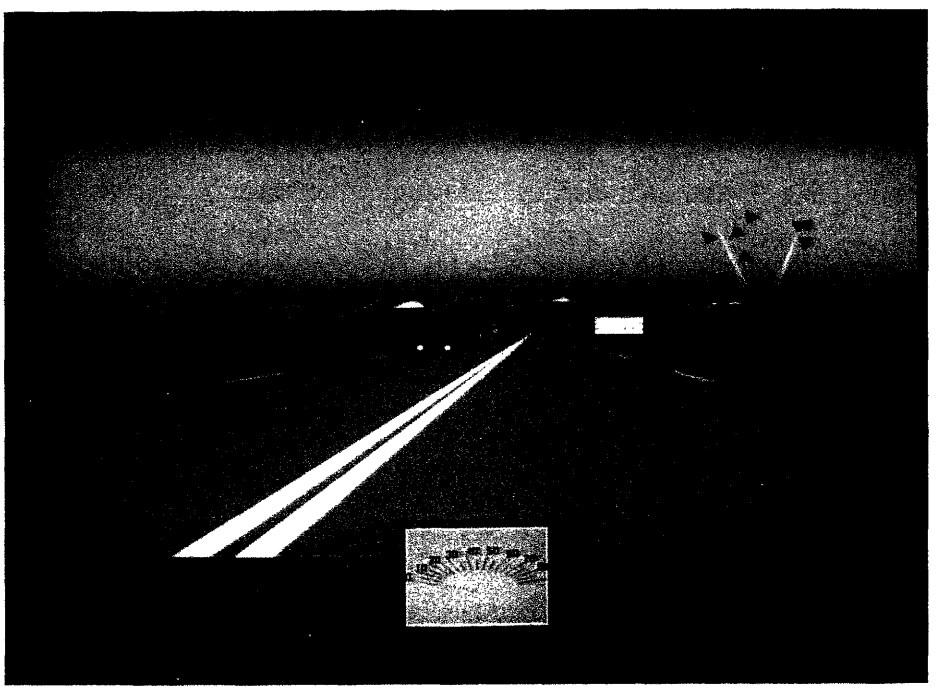

Figure A-2: Typical View from HMSL simulator

A.2.2 Control Feel

The control force or "feel" characteristics of steering and pedals can be an important aspect of simulator realism and impressions of the vehicle's handling and braking qualities can have small effects on driver performance. The primary concern in a car simulator is with the steering dynamics. The driver's hands and arms combined with the steering system should form a fairly complicated dynamic system with equivalent inertia, damping and compliance properties to those in real driving [34]. The driver controls the position of the steering wheel and receives proprioceptive feedback information on joint position and force exerted via pressure and stretch receptors. The driver's neuromuscular system also contains feedback loops or reflex arcs which operate with very small loop time delays of approximately 25 msec [35].

Due to current predominance of power-assisted steering, passive steering feel characteristics (i.e., spring, viscous damping, and friction) can offer a plausible steering feel. However, to correctly simulate the restoring torque reflected back by rolling tires on the road or the dynamics of power steering is more difficult. The HMSL simulator simulates the conventional steering system with motor-generated force feedback as a function of steering wheel position and vehicle speed. The control feel is controlled by a computer-driven fuzzy-logic controller.

Figure A-3 shows the setup of the springs for the gas and brake pedals and the motor for the steering wheel.

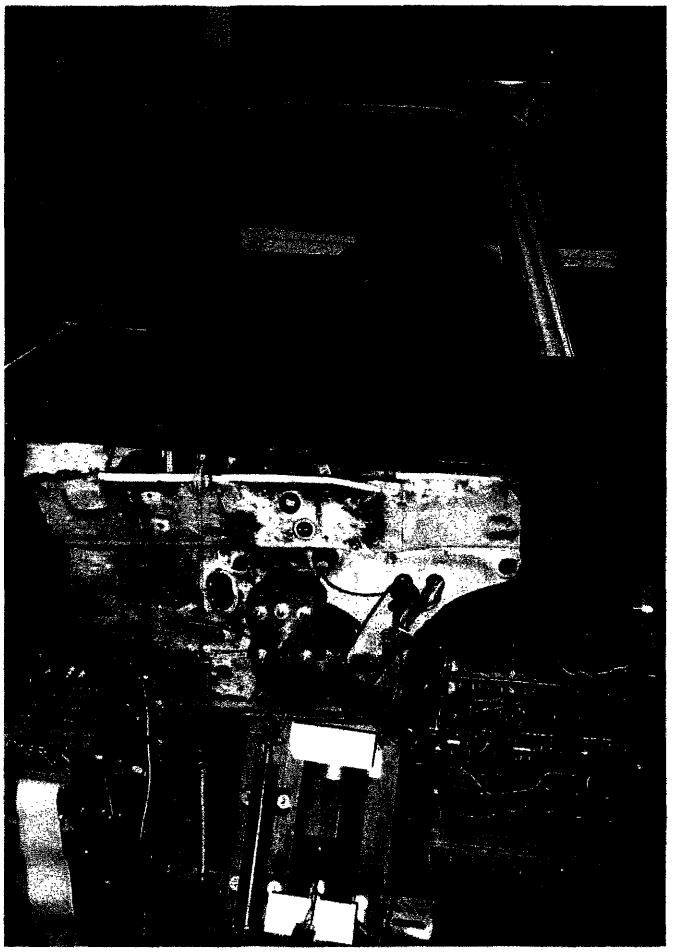

Figure A-3: Setup for the Gas and Brake Pedals and the Steering Wheel

A.2.3 Dynamics Computations

Driver control signals and driving scenario event commands are translated into commands for the driver interface systems via dynamic computations. The basic computations consist of the vehicle equations of motion, which generate vehicle accelerations and velocities as a function of control commands (gas, brake pedal position and steering wheel angle) and scenario inputs (road friction, wind gusts, downhill, etc.). Outputs from these equations command the motion and feel systems and auditory cue generator. The vehicle velocities are then integrated in kinematic computations

to yield vehicle state variables (e.g., distance, heading and lane position) which form commands to the display generator.

The equations of motion include force and moment expressions which in general would result in six-degree-of-freedom motions. Simplifications are usually applied here, however, as appropriate to a given situation, in order to minimize the development effort, improve reliability, and reduce cost. Computational delay is another concern in determining the degree of complexity of the equations of motion. At best, significant computational delay will reduce simulator realism. At worst, it will seriously destabilize the driver's closed-loop control behavior and invalidate experimental results.

The HMSL simulator uses Dugoff's vehicle model for the equations of vehicle motion [36]. Figure A-4 shows the overall model developed for this simulator. Dynamics of both the vehicle body and tires are taken into account in this model.

The equations of motion based on above model is described as follows. For the dynamic equations:

$$m(\dot{u} - rv) = F_x \tag{A.1}$$

$$m(\dot{v} - ru) = F_y \tag{A.2}$$

$$I\dot{r} = T \tag{A.3}$$

$$I_{wy}\dot{\omega} = T_i + F_{xwi}(R - \delta_{zi}) - F_{zi}X_{zi} - C_{wi}\omega_{wi} \tag{A.4}$$

$$F_x = F_{x1} + F_{x2} + F_{x3} + F_{x4} - F_D \tag{A.5}$$

$$F_y = F_{y1} + F_{y2} + F_{y3} + F_{y4} \tag{A.6}$$

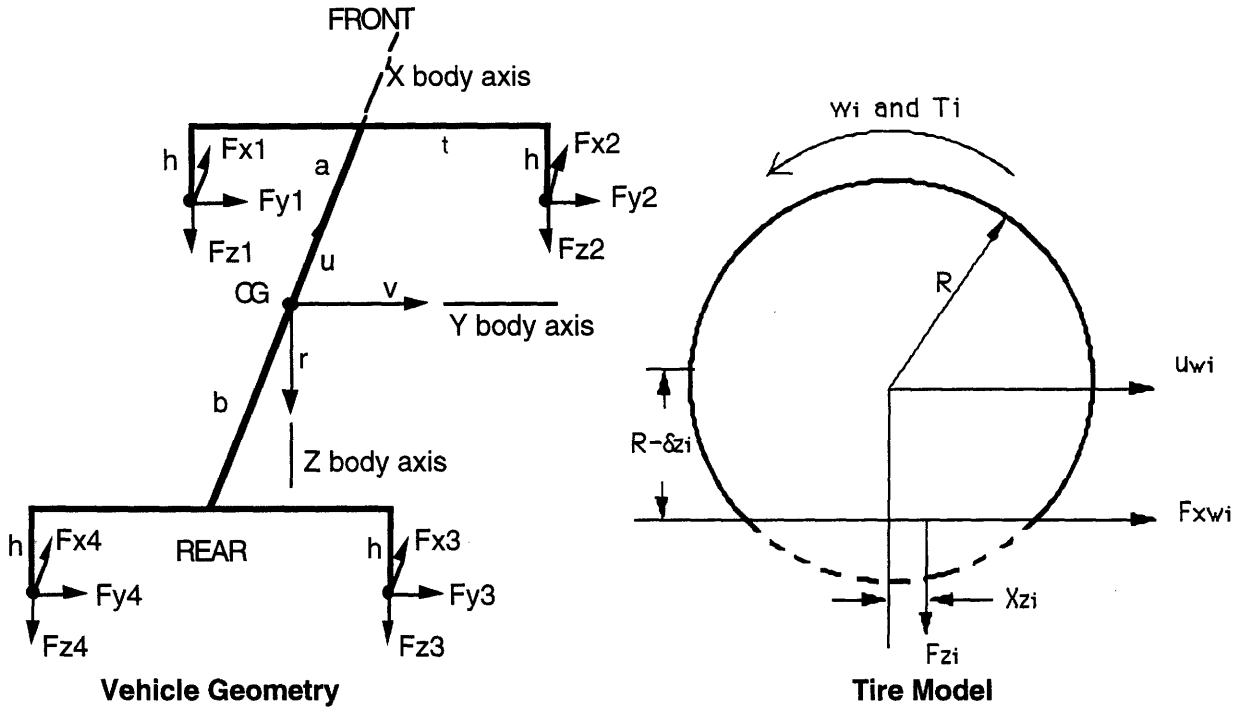

Figure A-4: Configuration of HMSL Driving Simulator Vehicle Model

$$T = t(F_{x1} - F_{x2} - F_{x3} + F_{x4}) + a(F_{y1} + F_{y2}) - b(F_{y3} + F_{y4}) \tag{A.7}$$

$$F_{xi} = F_{xwi}\cos(\delta_i) - F_{ywi}\sin(\delta_i) \tag{A.8}$$

$$F_{yi} = F_{xwi}\sin(\delta_i) + F_{ywi}\cos(\delta_i) \tag{A.9}$$

$$F_D = \frac{1}{2}C_D\rho A_D u^2 \tag{A.10}$$

For the tire kinematics:

$$u_1 = u + tr \qquad v_1 = v + ar \tag{A.11}$$

$$u_2 = u - tr \qquad v_2 = v + ar \tag{A.12}$$

$$u_3 = u - tr \qquad v_3 = v - br \tag{A.13}$$

$$u_4 = u + tr \qquad v_4 = v - br \tag{A.14}$$

$$u_{wi} = u_i\cos(\delta_i) + v_i\sin(\delta_i) \tag{A.15}$$

$$s_i = 1 + \frac{\omega_i R_{ei}}{u_{wi}} \tag{A.16}$$

$$\alpha_i = tan^{-1}\frac{v_i}{u_i} - \delta_i \tag{A.17}$$

A.2.4 Auditory Display

Auditory cues can be important feedback in certain control situations, such as tire squeal during cornering and braking, and in holding constant speed. In the real world these effects contain combined auditory and motion cues, which can be simulated to a large degree with auditory cues from a good sound system. Auditory cues can also add to driving realism through sounds associated with the engine, tires, wind, body resonance due to road texture, etc.

Auditory cues can be displayed with reasonable cost high-fidelity systems, and generated with a variety of sound generator electronics currently produced for video games. The more difficult job is to correctly generate the appropriate amplitude and frequency commands for realistic sound cues.

The HMSL simulator uses a PC-based SoundBlaster-Pro sound board to simulate all the sound effects for the simulator. FM sound is used to generate the engine noise as a function of engine speed. Digitized sound, on the other hand, is used to generate special sound effects such as tire squeal, car crash and car-passing sounds as a function of relative distance and speed. Generally speaking, these simple sound effects have been found to be satisfactory for the purpose of this research.

Appendix B

Analytical Basis of the Car-following Model

B.1 Kinematics of the Crash Scenario

The model considered in this thesis consists of two vehicles, lead vehicle A and following vehicle B, with the condition that the driver of the lead vehicle suddenly applies his/her vehicle's brakes. The driver of the following vehicle reacts to this situation and applies his/her own vehicle's brakes. There are several possible outcomes of these actions:

1. Vehicle B strikes moving vehicle A after vehicle B applies the brakes.

2. Vehicle B strikes stationed vehicle A after vehicle B applies the brakes.

3. Vehicle B strikes moving vehicle A prior to the time vehicle B applies the brakes.

4. Vehicle B strikes stationed vehicle A prior to the time vehicle B applies the brakes.

5. Vehicle B does not strike vehicle A.

Time equaling zero is assigned to the time at which the driver of vehicle A begins to apply his/her brakes. By applying the laws of motion it is possible to determine which of the above outcomes has occurred.

For vehicle A:

$$T_{AS} = V_A/\alpha_A, \tag{B.1}$$

$$S_A = V_A T_{AS} - \frac{1}{2}\alpha_A (T_{AS})^2, \tag{B.2}$$

where

T_{AS} = time in seconds required for vehicle A to stop given that it is not struck by vehicle B,

V_A = initial velocity of vehicle A in meters per second (mps),

α_A = brake deceleration in meters per second square (we have adopted the convention of assigning deceleration a positive sign, thus expressing it as a variable operating counter to velocity),

S_A = distance in meters covered by vehicle A during the time required to stop.

For vehicle B:

$$T_{BS} = V_B/\alpha_B, \tag{B.3}$$

$$S_B = V_B T_{BS} - \frac{1}{2}\alpha_B (T_{BS})^2, \tag{B.4}$$

where T_BS, V_B, α_B and S_B are corresponding variables for vehicle B.

The following distance between the two vehicles at time zero is D_f.

The instantaneous distance between vehicles can be determined from the following relations:

$$D(t_i) = S_A(t_i) + D_f - S_B(t_i), \tag{B.5}$$

$$D(t_i) = V_A t_i - \frac{1}{2}\alpha_A(t_i)^2 + D_f - V_B t_i - \frac{1}{2}\alpha_B(t_i - T_r)^2, \tag{B.6}$$

where

t_i = instantaneous time in seconds measured from time zero,

$D(t_i)$ = distance in meters between the two vehicles at time = zero,

T_r = braking reaction time in seconds for driver of vehicle B.

If $D(t_i)$ is less than or equal to zero, a crash has occurred . The time (t_c) at which a crash occurs can be determined by setting $D(t_c) = 0$ and solving for t_c.

$$t_c = \frac{1}{2\alpha_r}\{-V_r \pm [V_r^2 + 4\alpha_r D_r]^{\frac{1}{2}}\}, \tag{B.7}$$

where

$V_r = V_B + T_r\alpha_B - V_A$,

$\alpha_r = \frac{1}{2}(\alpha_B - \alpha_A)$,

$D_r = D_f + \frac{1}{2}(\alpha_B T_r^2)$.

The solution is the smallest positive value of t_c. An imaginary solution for t_c would imply that vehicles do not crash (i.e., the relative distance between does reach

zero). Thus the condition for a non crash is :

$$V_r 2 + 4\alpha_r D_r \leq 0. \tag{B.8}$$

If this condition is not met, then a crash has occurred. Note that equation (6) applies only when both vehicles are in motion and both have started to decelerate. Therefore, if t_c is less than T_r, a crash occurred before vehicle B began to decelerate. In this case, equation (6) becomes:

$$D(t_i) = V_A t_i - \frac{1}{2}\alpha_A (t_i)^2 + D_f - V_B t_i. \tag{B.9}$$

Again a crash occurs when $D(t_i) = 0$. Equation (9) can be used to solved for the time (t_i).

Note that the condition in which the following vehicle B stops before striking vehicle A was eliminated by an imaginary solution to equation (7). From the above results, the distance to crash point could also be computed.

B.2 Possible Analytical Solution

If it is desired to determine the probability of a crash analytically, one could begin with equation (8). Define a new variable:

$$\theta_1 = \theta_r = V_r 2 + 4\alpha_r D_r, \tag{B.10}$$

and compute its probability density function. Then,

$$probability\ of\ a\ crash\ = 1 - pr(\theta_1 \leq 0) = 1 - \int_{-\infty}^{0} f(\theta_1) d\theta_1. \tag{B.11}$$

One can conceptually obtain the density function of θ_r by a convolution of the distribution of the input variables [37]. The variables in (10) can be expressed in terms of the input variables as follows:

$$\begin{aligned} V_r &= V_B + T_r\alpha_B - V_A, \\ \alpha_r &= \tfrac{1}{2}(\alpha_B - \alpha_A), \\ D_r &= D_f + \tfrac{1}{2}(\alpha_B T_r^2). \end{aligned} \tag{B.12}$$

Therefore,

$$\theta_1 = g(D_f, T_r, \alpha_A, \alpha_B, V_A, V_B), \tag{B.13}$$

where g contains six independent random variables (ideal condition). These random variables are distributed as follows:

$$g(D_f, T_r, \alpha_A, \alpha_B, V_A, V_B) = f(D_f)f(T_r)f(\alpha_A)f(\alpha_B)f(V_A)f(V_B). \tag{B.14}$$

Five new random variables can be defined as:

$$\theta_i = f(D_f, T_r, \alpha_A, \alpha_B, V_A, V_B).(i = 2, 3, \cdots, 6) \tag{B.15}$$

The original variables can be transformed to functions of the θ_i's by using equation (15).

$$\begin{aligned} D_f &= D_f(\theta_1, \theta_2, \cdots, \theta_6), \\ T_r &= T_r(\theta_1, \theta_2, \cdots, \theta_6), \\ &\vdots \\ V_B &= V_B(\theta_1, \theta_2, \cdots, \theta_6), \end{aligned} \tag{B.16}$$

Using these variables we can write:

$$h(\theta_1, \theta_2, ..., \theta_6) = f[D_f(\theta_1, \theta_2, \cdots, \theta_6), T_r(\theta_1, \theta_2, \cdots, \theta_6), \cdots, V_B(\theta_1, \theta_2, \cdots, \theta_6)]|J|, \tag{B.17}$$

where $|J|$ is the absolute value of the Jacobian of the transformation. The distribution of θ_1 can be obtained by integration of (17).

$$h(\theta_1) = \int_{-\infty}^{\infty} \cdots \int_{-\infty}^{\infty} h(\theta_1, \theta_2, ..., \theta_6) d\theta_2 d\theta_3 \cdots d\theta_6. \tag{B.18}$$

If the distributions of the input variables in equations (14) can be expressed in convenient analytic form, it might be possible to perform the integration in equation (18). However, for this thesis, they are expressed as discrete distributions obtained empirically. At this point, the difficulties of obtaining an analytical solution should become evident. In addition, if one wishes to obtain a probability distribution of crash margin, as is done using the simulation model CARMASS, the problems become even greater. Therefore, the Monte Carlo simulation was chosen for this thesis.

Appendix C

Fuzzy Set Theory

C.1 Fuzzy Set

Traditionally, mathematics dictate that an object be only a full member of a given set, or not a member at all. There is nothing in between. What distinguishes fuzzy sets from conventional crisp sets is the fact that fuzzy set theory allows degrees of membership, varying from 0 (non-member) to 1 (full member). Fuzzy sets provide an elegant mechanism to describe and handle all sorts of so-called linguistic variables, the variable "speed" for instance. A linguistic variable is characterized by a series of terms, such as "low", "moderate" or "high", each term representing a fuzzy set (e.g. the fuzzy set "high speed", of which a speed of 80 km/hr may be a member to a degree of only 0.3). The function that associates a grade of membership of a fuzzy set with every object that to some extent could be in that set, is called the membership function. The most commonly used membership function is that of a

trapezium. Other examples are triangle, square, exponential, etc. When smoothness of the membership functions is considered essential, exponential relationships are employed.

C.2 Notation, Terminology and Basic Operation

A fuzzy set A of a universe of disclosure U is characterized by a membership function $\mu_A \rightarrow [0,1]$, which associates with each element y of U a number $\mu_A(y)$ in the interval [0,1], which represents the grade of membership of y in A. The support of A is the set of points in U at which $\mu_A(y) > 0$. A fuzzy singleton is a fuzzy set whose support is a single point in U. In particular, A is called a non fuzzy singleton if the grade of the only element is 1.

Let A and B be two fuzzy sets in U with membership functions μ_A and μ_B, respectively. The set theoretic operations of union and intersection for fuzzy sets are defined as follows. The membership function $\mu_{A \cup B}$ of the union $A \cup B$ is pointwise defined for all $u \in U$ by

$$\mu_{A \cup B}(u) = max(\mu_A(u), \mu_B(u)). \tag{C.1}$$

The membership function $\mu_{A \cap B}$ of the intersection $A \cap B$ is pointwise defined for all $u \in U$ by

$$\mu_{A \cap B}(u) = min(\mu_A(u), \mu_B(u)). \tag{C.2}$$

For a detailed discussion of fuzzy sets and operations on fuzzy sets, refer to Zadeh

[38].

C.3 Fuzzy-Logic Controller

A comprehensive survey of fuzzy-logic controller (FLC) design has been made by Lee [39]. In the following section, the author will review the most common type of FLC. It was employed by Holmblad and Osterggard [28].

As shown in figure C-1, an FLC consists of the following major units. Fuzzy reasoning is performed by the inference engine, the kernel of the FLC. The fuzzification inference converts real numbers into fuzzy sets, to be supplied as an input to the decision making logic. The knowledge base of an FLC comprises two components, namely, a data base and a fuzzy control rule base. The data base provides the inference engine with the membership functions of fuzzy sets used in the rule base. The rule base holds the control rules. The defuzzification inference transforms fuzzy control actions into non fuzzy, crisp controls. Fuzzification is performed by interpreting an input x_0 as a non fuzzy singleton A, that is, $\mu_A(x_0)$ is equal to zero, except at the point x_0, at which $\mu_A(x_0)$ equals one. The antecedent part of a control rule consists of a number of conditions, each of them relating an input to a term which is represented by a fuzzy set ("speed is high" for example). Analogously, the antecedent consists of one or more conclusions. Control rules, just as the contents of the data base, are usually formulated by consulting experts. The so-called self-organizing controller [40], however, is an exception to this rule. For a self-organizing controller, it is not necessary to have an exhaustive set of rules as the starting point. By applying

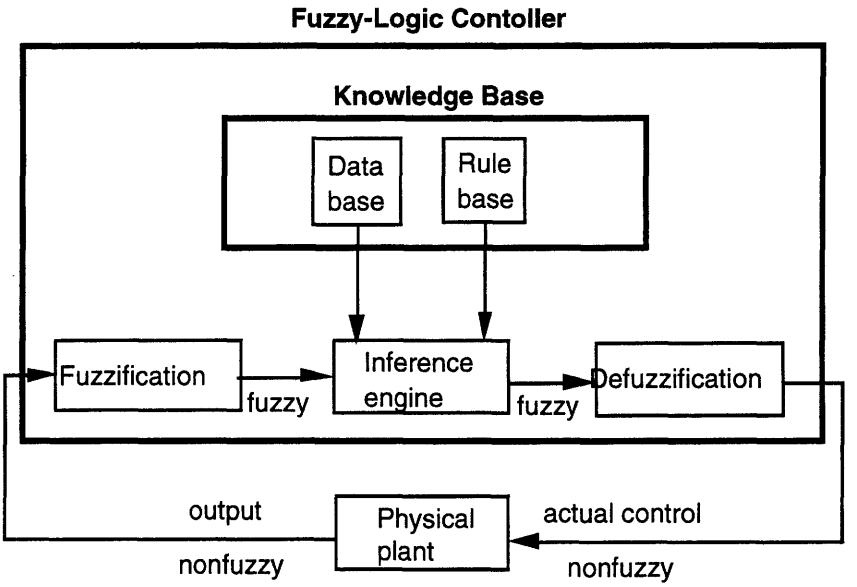

Figure C-1: Configuration of Fuzzy-Logic Controller

a performance criterion, the algorithm is capable of conceiving additional rules, and of deleting redundant or contra-productive rules.

In order to illustrate the operation of the inference mechanism, consider the following dual-inputs-single-output mechanism of n fuzzy control rules:

$$\begin{aligned} &input: && x \text{ is } A' \text{ and } y \text{ is } B' \\ &rules: && if\ x \text{ is } A_i \text{ and } y \text{ is } B_i \text{ then } C_i \\ &output && z \text{ is } C' \end{aligned} \tag{C.3}$$

where x, y and z are linguistic variables representing the process state variables and the control variables, respectively. A_i, B_i and C_i, on the other hand, are linguistic values (or terms) of the linguistic variables x, y and z in the universe of disclosure U, V and W, respectively, with $i = 1, 2, ..., n$. The inference process starts with assessing for every rule the weighting factors α_i that express the significance of that rule. Since

non fuzzy singletons are assumed for a defuzzification strategy (i.e., the fuzzy inputs A' and B' are equal to the non fuzzy input x_0 and y_0, respectively), this may simply be performed as:

$$\alpha = \mu_{A_i}(x_0) \wedge \mu_{B_i}(y_0) \tag{C.4}$$

with $i = 1, 2, ..., n$, and where $\mu_{A_i}(x_0)$ and $\mu_{B_i}(y_0)$ play the role of the degrees of partial match (per condition) between the controller input and the corresponding term in the i^{the} rule. The contribution of the i^{the} rule to the fuzzy controller output is then calculated as:

$$\mu_{C_i'}(w) = \alpha_i \mu_{C_i}(w) \tag{C.5}$$

As a result, the membership function $\mu_{C'}$ which is the union of the individual control decisions C.5, is

$$\mu_{C'}(w) = \bigcup_{i=1}^{n} \alpha_i \mu_{C_i}(w) \tag{C.6}$$

Deducing a crisp control value z_0 from C' is achieved by performing one of two defuzzification strategies. The first method, "center of area" or "zero-order moment" method, calculates the abscissa value that divides the area under the output membership function in two equal parts. The other method, "center of gravity" or "first-order moment" method, yields the center of gravity of the output membership function.

Appendix D

Fuzzy-Logic Intelligent Cruise Control

The fuzzy-logic intelligent cruise controller was designed by referring to the human operator's experience and to control engineering knowledge. The design procedure for the fuzzy-logic braking controller will be described in detail in the following sections.

D.1 Control Scheme

For the car-following controller, the following variables were used as input information.

D : relative distance between own car and lead car

V : absolute speed of own car

R : relative speed between own car and lead car

We assumed that we have perfect sensors and actuators, i.e., the dynamics of them were ignored. Based on this information and the knowledge extracted from a hypothetical expert driver, the controller determines appropriate control action.

B : braking torque

T : engine torque

The following are some possible rules we could expect from an expert:

1. *If absolute speed is fast and distance is large and lead car is opening then increase engine power slightly;*

2. *If absolute speed is fast and distance is large and lead car is closing then decrease engine power slightly;*

3. *If absolute speed is medium and distance is small and lead car is closing then apply medium braking;*

4. ...

Note that only one output can be used each time. Therefore additional rules are needed to avoid any conflicts. For example, we added "if there is braking then exert no engine torque output."

Figure (D-1) shows the block diagram of this controller.

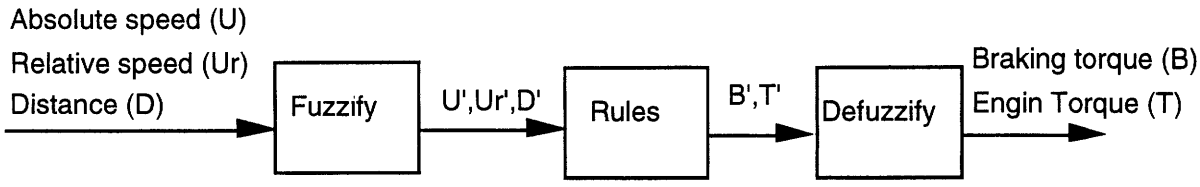

Figure D-1: Block Diagram for Car-following Controller

D.2 Input Fuzzification

Figure (D-2) shows one example of the partition of the input spaces. Note that the δ is the desired car-following distance derived from the safe car-following distance distribution which is adjustable.

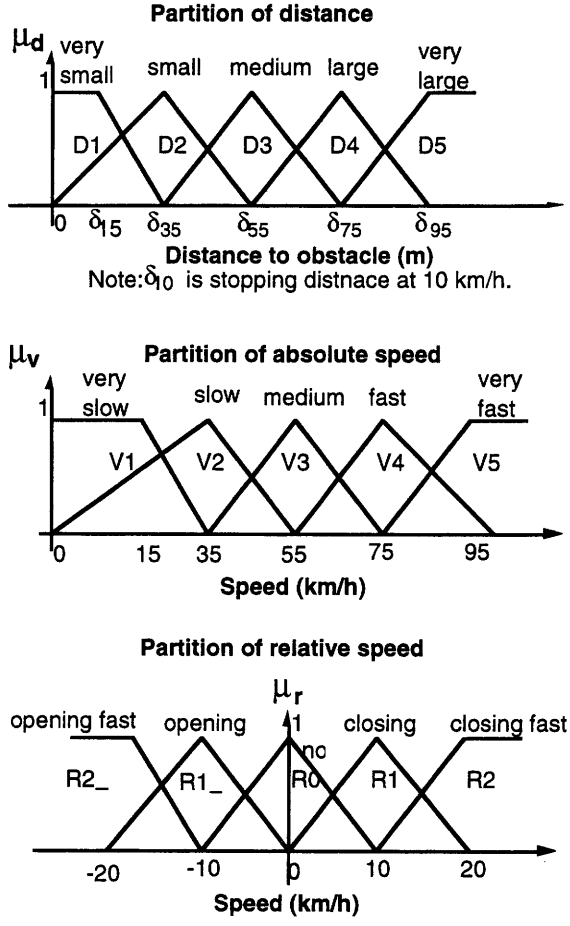

Figure D-2: Input Membership Functions for Car-following Controller

D.3 Fuzzy Rules

Since there are three inputs for this controller, there is no way to express all the fuzzy rules in a simple matrix form such as that for the braking controller. In this preliminary design, we use five partitions for for each input. This results in 125 rules for the whole controller, which is somewhat complex to derive immediately and required numerous iterations to get to the final rule base.

D.4 Output Defuzzification

Figure (D-3) shows the combination of the output membership functions. The range of the braking torque is 0 - 1800 Nm while the increase/decrease of engine torque is limited to 200 Nm. Note that the two outputs are mutually exclusive, i.e., if braking is used, the engine power must be cut off, and vice versa.

The final crisp output was determined using the center of gravity method. For instance, for the braking output, the output torque would be:

$$Output\ torque = \frac{\sum_{i=0}^{3}(\mu_i \cdot B_i)}{\sum_{i=0}^{3}\mu_i} \tag{D.1}$$

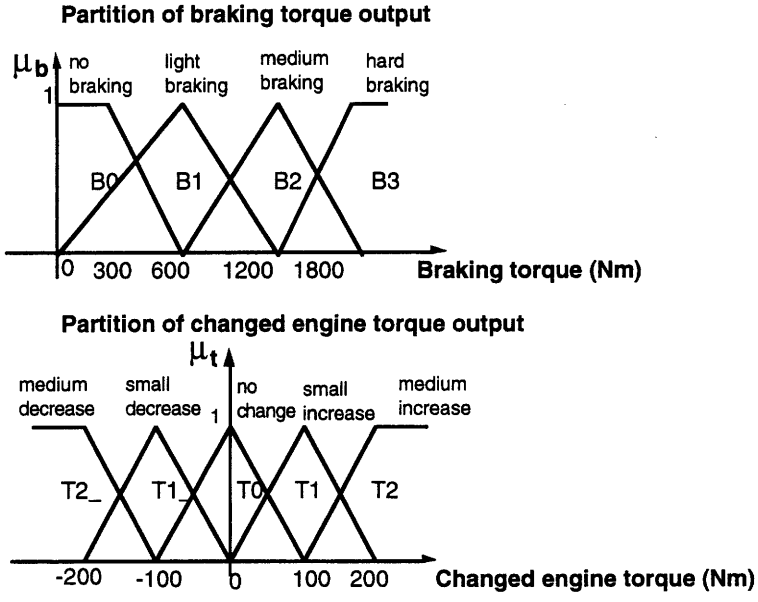

Figure D-3: Fuzzy Rules for Braking Controller

Bibliography

[1] Accident Facts. National Safety Council, Itasca, IL, 1992.

[2] McGehee, D.V., Dingus T.A. and Horowitz A.D. The potential value of a front-to-rear- end collision warning system based on factors of driver Behavior, visual perception and brake reaction. In *Proc. of the Human Factors Society 36th Annual Meeting,* Atlanta, 1003-1005, 1992.

[3] Tolle, J. E. Vehicular headway distribution: testing and results. In *Transportation Research Record,* 456, 56-64, 1976.

[4] Koshi, M., Iwasaki M. and Ohkura I. Some findings and an overview on vehicular flow characteristics. In *Proc. of the 8th International Symposium on Transportation and Traffic Flow Theory,* 1981 (edited by Hurdle V.F., Hauer E. and Stewart G.N.) University of Toronto Press, Toronto, Ontario, 403-426, 1983.

[5] Chishaki, T and Tamura Y. Headway distribution model based on the distinction between leaders and followers. In *Transportation and Traffic Theory,* 43-63, 1984

[6] Dull, E.H. and Peters H.J. Collision avoidance system for automobiles. SAE paper 780163, 1978.

[7] Ioannou, P.A., Chien C.C. and Hause J. Autonomous intelligent cruise control. In *Proc. of the IVHS America 1992 Annual Meeting,* Newport Beach, California, 1, 97-105, 1992.

[8] Colbourn, C.J., Brown I.V. and Copeman A.K. Drivers' judgements of safe distances in vehicle following. In *Human Factors,* 20(1), 1-11, 1978.

[9] Fenton, R.E. A headway safety policy for automated highway operations. In *IEEE Transaction on Vehicular Technology,* VT-28, 1, 22-28, 1979.

[10] Minami, K., Yasuma, T. and Okabayashi, S. A collision-avoidance warning system using laser radar. SAE paper 881859, 1988.

[11] Morita, T. An approach to intelligent vehicle. In *Proc. of the Intelligent Vehicles,* 1993.

[12] Ioannou, P., Xu, Z., Eckert, S., Clemons, D. and Sieja, T. Intelligent cruise control: theory and experiemnt. In *Proceeding of 32 CDC,* San Antonio, TX, 1885-1890, 1993.

[13] Kakinami T., Sato J., Saiki, M. and Soshi K. Autonomous vehicle control system using an image processing sensor. SAE paper 950470, 1995.

[14] Gortan, L., Borodani, P. and Carrea P. Fuzzy-logic employed in an autonomous ICC vehicle. SAE paper 950472, 1995.

[15] Wasielewski, P. Car-following headways on highways interpreted by semi-Poisson headway distribution model. In *Transportation Science,* Vol.13, No.1, February 1979.

[16] Schwartz, S. H., Allen, R. W., Hogge, J. R. and Stein, A. C. A simulator study of driver reaction to metric speed sign. In *International Symposium on Traffic Control System,* Berkeley, 1979.

[17] Yoshimoto, K. An analysis of the man-automobile system with a driving simulator. In *Proceeding of IFAC Conf. on Man-Machine Systems,* Baden-Baden, Germany, 1982.

[18] Malaterre, G. and Lechner, D. Emergency manoeuvres at junctions using a driving simulator. In M. Koshi (Ed.) *Transportation and Traffic Theory,* North-Holland: Elsevier Science Publishing Co., Inc., 1990.

[19] Kappler, W. Using a driving simulator to investigate vehicle handling properties. In H.P. Willumeit (Ed.) *Human Decision Making and Manual Control,* North-Holland: Elsevier Science Publishing Co., Inc., 1986.

[20] Farber, E. and Paley, M. Using freeway data to estimate the effectiveness of rear-end collision countermeasures. In *Proceeding of IVHS America 1993 Annual Meeting,* Washington D.C., 1993.

[21] Johansson, G. and Rumar, K. Drivers' brake reaction time. In *Human Factors,* 13(1), 23-27, 1971.

[22] National Highway Traffic Safety Administration Rear-end crashes: problem size assessment and statistical description(DRAFT), Office of Crash Avoidance Research, NHTSA, December 2, 1992.

[23] Olson, P.L. and Sivak, M. Perception-response time to unexpected roadway hazard. In *Human Factors,* 28(1), 91-96, 1986.

[24] Clarke, R.M., Goodman, M.J., et al. Driver performance and IVHS collisions avoidance systems: a search for design-relevant measurement protocols. In *Proceeding of IVHS America 1993 Annual Meeting,* Washington D.C., 1993.

[25] Knipling, R.R., Hendricks, D.L., et al. A front-end analysis of rear-end crashes. In *Proceeding of IVHS America 1992 Annual Meeting,* Newport Beach, Calif., 1992.

[26] Zadeh, L.A. Fuzzy algorithm. In *Information and Control,* V8, p338-353, 1965.

[27] Kosko, B. *Neural Networks and Fuzzy Systems.* Prentice-Hall, New Jesey, 1991.

[28] Holmblad, L.P. and Ostergaard, J.J. Control of a cement kiln by fuzzy logic. In M.M. Gupta and E. Sanchez (Eds.) *Fuzzy Information and Decision Process,* p389-399, Elsvier, Amsterdam, 1982.

[29] Ren, J. and Sheridan, T.B. Optimization with fuzzy linear programming and fuzzy knowledge base. In *Proc. of IEEE World Congress on Computational Intelligence,* Orlando, Florida, 1994.

[30] Mamdani, E.H. Application of fuzzy logic to approximate reasoning using linguistic systems. In *IEEE Trans. Comput.,* nr.26, p1182-1191, 1977.

[31] Donges, E. A two-level model of driver steering behavior. In *Human Factors,* Vol. 20, No. 6, p691-707, December 1978.

[32] Gordon, D.A. Perceptual basis of vehicular guidance. In *Public Roads,* Vol. 34, No. 3, p53-68, 1966.

[33] McRuer, D.T. and Klein, R.H. Comparison of human driver dynamics in simulators with complex and simple visual displays and in an automobile on the road. In *Eleventh Annual Conference on Manual Control,* NASA TMX-62, 464,p684-692, 1975.

[34] Jex, H.R. and Magdaleno, R.E. Biomechanical models for vibration feedthrough to hands and head for a semisupine pilot. Presented at *Symposium on Biodynamic Models and Their Applications,* February 1977.

[35] Gualtierotti, T., Spinelli, D. and Margaria, R. Effect of stress on lower neuror activity. In *Experimental Medicine and Surgery,* Vol. 26, Nos. 2-3, 1958.

[36] Dugoff, H., Fancher, P.S., and Segel, L. An analysis of tire traction properties and their influence on vehicle dynamic performance. SAE paper 700377, 1970.

[37] Hogg, R.V. and Craig, A.T. *Introduction to Mathematical Statistics.* 3rd Edition, The macmillan Co., Toronto, 1970.

[38] Zadeh, L.A. Outline of a new approach to the analysis of complex systems and decision processes. In *IEEE Trans. Systems, Man and Cybernetics,* SMC-3, p28-44, 1973.

[39] Lee, C.C. Fuzzy logic in control system: fuzzy logic controller - part I & II. In *IEEE Trans. Systems, Man and Cybernetics,* SMC-20, p404-435, 1990.

[40] Procyk, T.J. and Mamdani, E.H. A linguistic self-organizing process controller. In *Automatica,* 15, p15-30, 1979.